MECN4006: MECHANICAL ENGINEERING RESERACH PROJECT

PERSONS GAIT CYCLE ANAYSIS USING SINGLE IMU SYSTEM

RESEARCH PROJECT CODE: ATK9

Student

Osca Kholopha

Course coordinator

Supervisor

A research project submitted to the Faculty of Engineering and the Built Environment, University of the Witwatersrand, Johannesburg, in partial fulfilment of the requirements for the degree of Bachelor of Science in Engineering. Johannesburg, 05 October 2024

ABSTRACT

This research investigates the use of a single Inertial Measurement Unit (IMU) embedded in an Android device to analyse human gait cycles in real-world conditions. Ethics approval was granted by the Human Research Ethics Committee (Non-Medical) at the University of the Witwatersrand (Clearance No. MIAEC 109/24W).

A mobile application model was developed to collect IMU data of acceleration, angular velocity, and orientation as well as GPS data for simultaneous motion tracking. GPS readings were used to validate displacement estimates derived from IMU integration, confirming the system's reliability in real-time movement analysis.

Data was collected across three gait categories, relaxed walking, fast walking, and jogging. Each category was sampled at a distinct rate to match its motion dynamics. 25 Hz for relaxed walking, 75 Hz for fast walking, and 100 Hz for jogging. The device was tested in two placements: inside the pocket and held by hand.
IMU signals were used to map the stance phases for the lower body and swing phases for the upper body of the gait cycle, forming the basis for gait identification. Jogging produced peak accelerations of 18.2 m/s² and stance durations averaging 0.32 seconds. Relaxed walking showed lower peak accelerations around 9.5 m/s² and longer stance durations near 0.58 seconds. Fast walking exhibited intermediate values, with stride intervals averaging 1.12 seconds. Despite increased signal noise in the handheld configuration, gait phase detection remained reliable.

These findings demonstrate that a single IMU, combined with adaptive sampling rates and GPS validation, can effectively distinguish gait types and phases. The system offers a low-cost, portable solution for gait analysis with applications in fitness tracking, health monitoring, and biometric identification. Future work will focus on broader demographic testing and machine learning integration.

AI DELCERATION

1. *Disclosure: Editing/refining grammar, spelling, formatting*

☒ I acknowledge the use of Quill Bot(https://quillbot.com/) and ChatGPT (https://chatgpt.com/) version GPT-3.5 2024, to improve the grammar. I pasted the text that I generated and formulated myself into the ChatGPT text box and entered the following prompt:

Original Prompt and Follow-up Prompt:
- Highlight grammatical errors in the pasted text.
- From the highlighted grammatical errors, suggest potential fixes.

Using the output from ChatGPT, I refined my original content for each part where I requested grammar corrections.

2. *Disclosure: Generated/manipulated image – list each occurrence*

☒ I acknowledge the use of RemoveBG(https://www.remove.bg/) and Fotor (https://www.fotor.com/ to remove background color and text from images used in my information resources. I used the mentioned tools to clean the sourced images by removing the background color, changing it to white so it would match the main document of my project. I have used them to erases text from the images and added only the text relevant to my design project to ensure that the formatting was consistent with the main document's text family and font size.

3. *Disclosure: Generated/manipulated– list each occurrence*

☒ I acknowledge the use of ChatGPT(https://chatgpt.com/) to debug MATLAB code that I created to identify any potential issues.

I entered my MATLAB code into the ChatGPT interface and used the following prompt

Original Prompt
- Review the provided code to identify any logical or mathematical errors

Based on my ability, I was able to critically evaluate whether the suggestions for my errors made sense and to determine if ChatGPT provided accurate debugging before I could change anything

☒ *I declare that the disclosure is complete and truthful.*

Student number: █████

Course code: MECN4005

Date:12/07/2024 to 05/10/2024

TABLE OF CONTENT

CONTENTS

LIST OF FIGURES

1 INTRODUCTION

1.1 Background and Motivation

Gait refers to the pattern of movement that enables locomotion. It involves a rhythmic series of leg movements that propel the body forward while conserving energy shown in Figure 2. The application of gait analysis has grown significantly, finding relevance in areas such as healthcare, sports science, security recognition systems, and fitness. This project focuses on gait analysis for recognition purposes [1, 2].

A number of studies have investigated gait analysis, including notable contributions from Chen et al [3]. and Gaud et al. [4]. These researchers employed different data collection methods for gait analyses, characterised into Non-Wearable Sensors (NWS), Wearable Sensors (WS), and Image Processing (IP). NWS and IP systems collect gait data in controlled environments with strategically placed sensors (refer to Figure 1a and Figure 1c). In contrast, WS systems offer more flexibility, allowing sensors to be positioned on different parts of the body such as the hips, knees, or feet to measure different aspect of gait (refer to Figure 1b).

a) NWS system   b) WS system   c) IP system
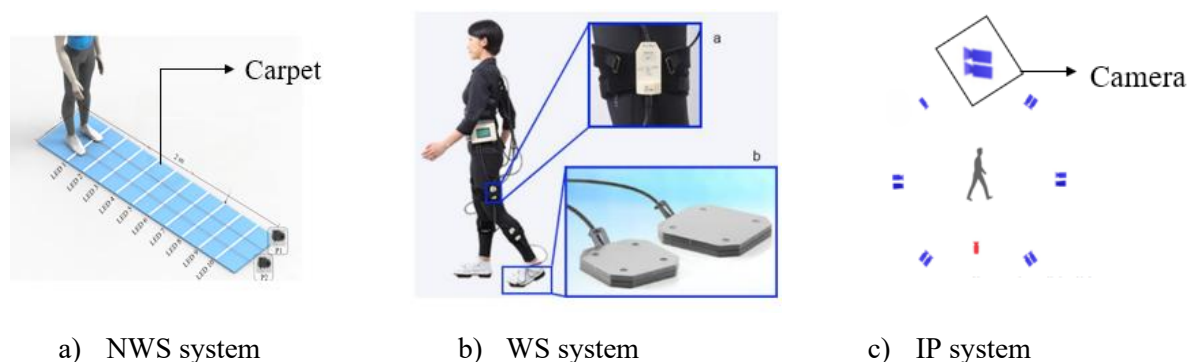
Figure 1:Different types of sensors for gait analyses [5, 6, 7]

NWS and IP systems are primarily designed for controlled environments, and they cannot be suitable for observing gait in daily situations. On the other hand, WS systems can collect data in real-life situation and provide insights into how individuals walk. However, a notable challenge with WS, as shown in Figure 1b, is that they impact the user's walking pattern and comfort. This issue can be mitigated using small devices with built-in Inertial Measurements Units which will be elaborated upon in the Biomechanics during gait cycle section

1.2 Literature Review

To examine and analyse walking patterns, understanding gait cycle which is defined as the sequence of movements from one foot strike to the subsequent foot strike on the same side is important for this study

[8]. This section will explore more on gait cycle, detailing how movements can be analysed and the distinctive gait cycle that can be identified through this analysis. These characteristics can be used for biometric identification to uniquely recognize individuals.

1.2.1   Person gait cycle

A complete gait cycle involves two distinct phases: the stance phase and the swing phase. Figure 2 illustrates the gait cycle of a walking person, highlighting the events occurring in each phase.
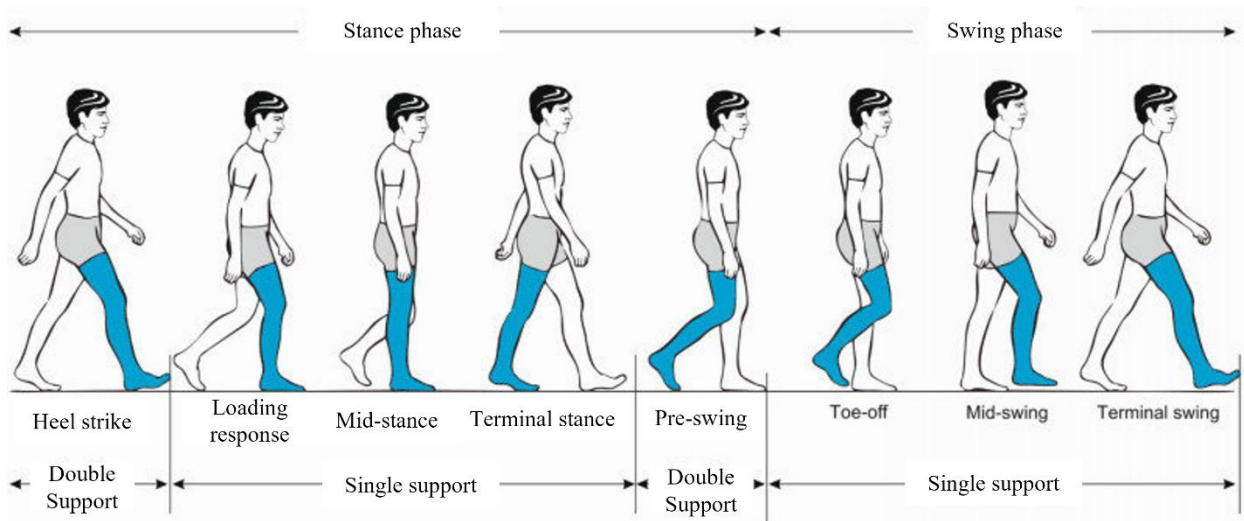
Figure 2:Complete gait cycle [9]

1.2.2   Stance and swing phase

Stance phase

As shown in Figure 2 above, a normal gait cycle begins and ends with the heel strike, which is when the leading foot first contacts the ground. This marks the start of the load response phase, during which the leading foot bears the body's weight as it fully contacts the ground. The heel strike and foot flat events are characterized by a rapid loading of the limb. During the double support phase, both feet are in contact with the ground, providing maximum stability. In the midstance phase, the body moves forward while the opposite leg enters the swing phase. This position is less stable due to the narrow base of support and the higher centre of gravity. The heel off event, where the heel lifts from the ground, signals the transition from midstance to terminal stance. In the terminal stance phase, the body continues to move forward until the pre-swing phase begins, leading to the toe-off event where the toes lose contact with the ground [10].

Swing phase

The swing phase then begins as the swinging leg moves forward past the stance leg, contributing to forward progression. This phase is divided into three sub-phases namely, the initial swing, where the leg accelerates

2

forward; the mid-swing, where the leg passes the opposite stance leg; and the terminal swing, where the leg decelerates in preparation for the next heel strike, which will end the swing phase [10].

The events in each part of the gait cycle help track the movement of the lower limb. They are important for identifying and distinguishing each step during walking. This swing and stance phases are used to specified different condition when modelling the human walking pattern. Other factor that are induced during the gait cycle are hip rotation and arm swing which are explained below

Hip rotation

Throughout the gait cycle, hip rotation shows distinct patterns influenced by both static and dynamic positions. During the stance phase, the hip starts in a neutral position at initial contact, then increases internal rotation as weight shifts onto the leg to accommodate ground forces. This internal rotation has a strong correlation with static hip rotation, suggesting that the resting position can help predict movement during walking. In midstance, the connection between static and mid-pivot rotations enhances balance and stability. As the gait transitions to terminal stance, the hip may begin to rotate externally in preparation for push-off. In the swing phase, the hip flexes while continuing to rotate internally to help clear the foot, and then it rotates externally near the end to align properly for the next step [11].

a) Femur rotation   b) Rotation during motion
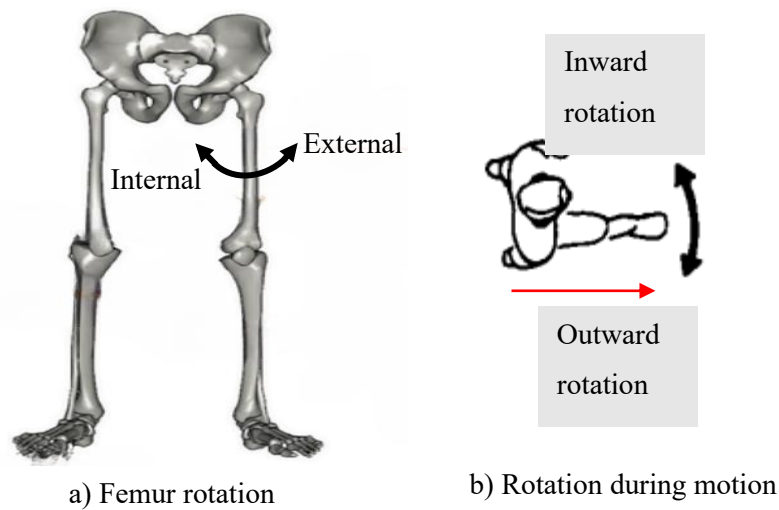
Figure 3:Hip rotation during gait cycle [26, 27]

Arm swing phases

The gait cycle, involving the lower limbs, also results in the movement of the upper body, specifically the arms. During walking, arm swinging can be classified into phases of swing based on their movement and angles relative to the legs. Figure below shows the definition of swinging of arms
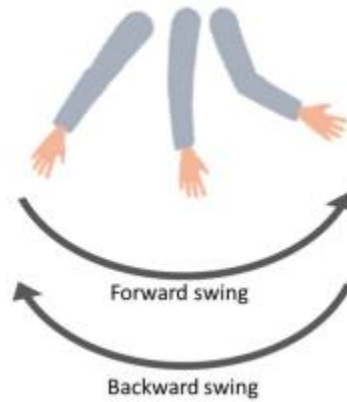
Figure 4:Swing movement of arm during gait cycle [12]

Studies have indicated that arm swing plays an important role in maintaining balance and improving energy efficiency during walking. The synchronized movement of the arms counteracts the leg movements as shown in Figure 5, contributing to stability throughout the gait cycle. As one leg advances, the opposite arm swings forward, providing a counterbalance that helps to prevent falling. This coordination is important for maintaining an upright posture. In terms of energy efficiency, the motion of the arms decreases the energy needed for walking by reducing the angular momentum produced by the legs. This lowered energy expenditure facilitates a more fluid walking pattern, allowing individuals to save energy over longer distances [13].

P1   P2   P3   P4   P5   P6   P7
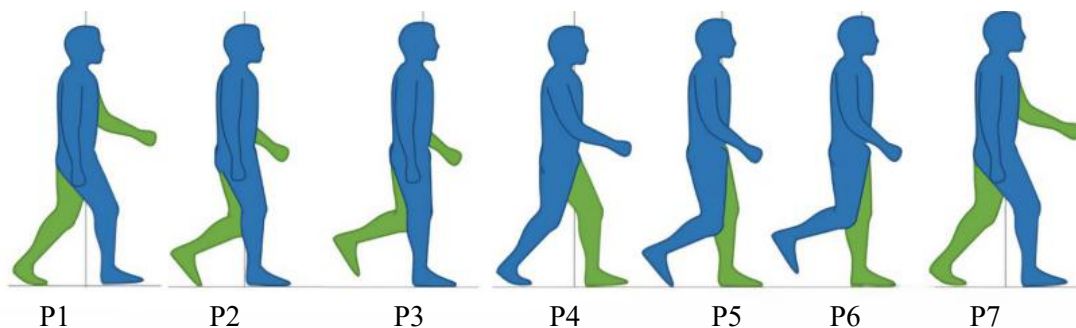
Figure 5:Arm swing movement during gait cycle [25]

During the gait cycle shown in Figure 5 above, the positions of the legs and corresponding arm movements are closely coordinated. At P1, when the right heel strikes, the left arm swings forward to maximum. At P2, as the left leg reaches maximum swing, the right arm also moves forward. When the left toe lifts off at

P3, the left arm begins to move back. In P4, the right arm transitions forward as the left leg enters mid swing. At P5, during right mid stance, the left arm moves back. This pattern continues: as the left heel strikes at P7, the right arm swings forward, and as the right leg reaches maximum swing at P8, the left arm mirrors this motion

1.2.3 Biomechanics during gait cycle

Gait analysis is based on two primary methods of system which are kinematics and kinetics [10]. Kinetics examines the forces involved in generating walking movements as shown below in Figure 6a. These forces are calculated from ground-reaction forces and then traced through the lower limbs and joints using biomechanical models. Kinematics (shown in Figure 6b) focuses on the movement of the body through space, analysing the position and motion of body segments and the angular displacements of joints.

a) Kinetic gait analysis   b) Kinematics gait analysis
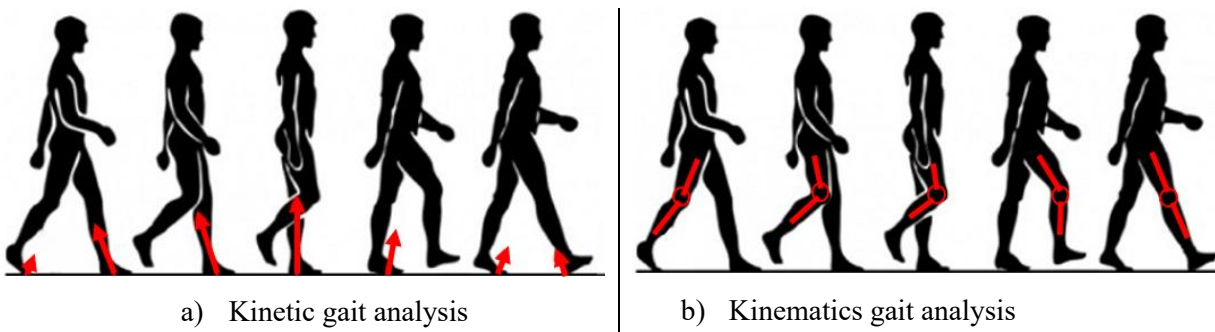
Figure 6:Different biomechanics analyses of gait cycle [14]

Both types of analyses in Figure 6 can be achieved using wearable sensor systems, which are advantageous due to their affordability and ease of integration to the human body and ability to be used outside laboratory or controlled environment which can be used in everyday real-life activities.

Kinetic and kinematics sensors

Figure 7 below shows different types of seniors and the placement to track the gait parameters.

a) Kinetic sensor   b) Kinematics sensor   c) Kinematics sensor
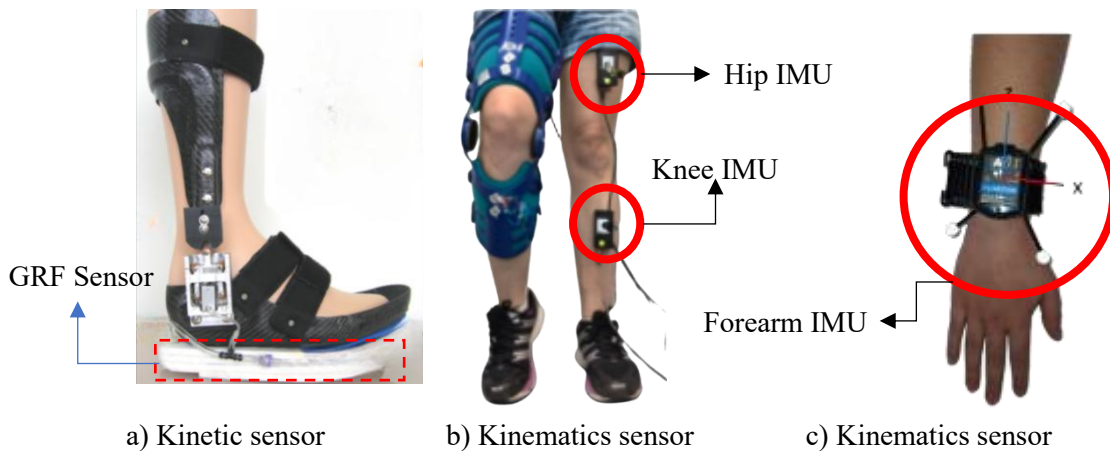
Figure 7: Sensors for Kinetics and kinematics motion [22, 23, 12]

5

For a comprehensive kinetic gait analysis, sensors are required to measure the ground reaction forces between the foot and the ground. The standard sensors used for this purpose are wearable Ground Reaction Force (GRF) sensors as shown in Figure 7a. In contrast, kinematic gait analysis as shown in Figure 7b and Figure 7c makes use of Inertial Measurement Units (IMUs). IMUs are preferred as they can be mounted on various body parts relevant to the study, such as the feet, hips, or femur, thereby offering a broad range of gait analysis. IMUs are commonly incorporated into wearable devices, including smartwatches and smartphones, which can be used during everyday activities without affecting the individual's walking pattern.

The use of GRF sensors will compromise the accuracy of gait analysis due to potential alterations in the user's walking pattern and comfort. GRF sensors are often integrated into shoes or insoles, which can interfere with the user's preferred footwear and overall comfort. Given these considerations, kinematic gait analysis using IMU is more suitable for this research project due to their minimal impact on the user's natural walking pattern and their flexibility in placement.

IMU Sensors for Gait Cycle

An Inertial Measurement Unit (IMU) is a device that combines several sensors to track different types of motion and orientation. It has accelerometers that measure acceleration along three axes, detecting changes in speed and direction. The IMU also includes gyroscopes that measure the rate of rotation around three axes, showing how the device or system is rotating. It also allows the measuring of the orientation of the device [15].

Accelerometer sensor in gait cycle

In gait analysis, an accelerometer sensor is used to measure the directional acceleration of motion. The acceleration recorded by the accelerometer corresponds to the body part on which the sensor is mounted. Figure 8a illustrates the accelerometer and the directions in which acceleration is measured. Figure 8b shows the movement of the person and the different axes involved (x, y, and z). The acceleration along these axes is denoted as $\ddot{x}$, $\ddot{y}$ and $\ddot{z}$ respectively.

| a) Accelerometer | b) Directional motion of human |
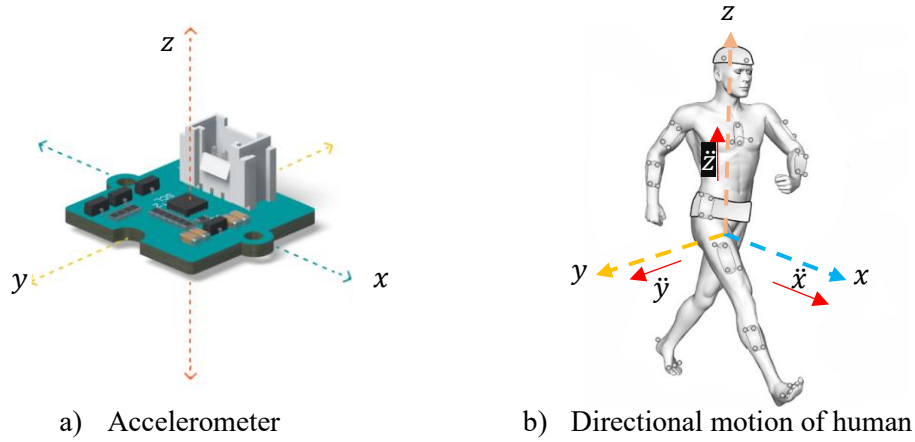
Figure 8:Acceleration sensor and the direction of human motion [16, 17]

Gyroscope sensor in gait cycle

Because some segments of the body where the IMU is mounted for gait analyses does not only translate but also rotates during movement, it is important to measure the angular velocity of specific body parts as they rotate around particular axes and the angle of rotation. As shown in the Figure 9 below, walking involves not only forward motion but also the rotational dynamics of the lower limb segments (thigh and shank) at their joints. This combination of translational and rotational movement contributes to the overall gait cycle, which is characterized by angular velocity.

| a) Gyroscope | b) Directional human motion |
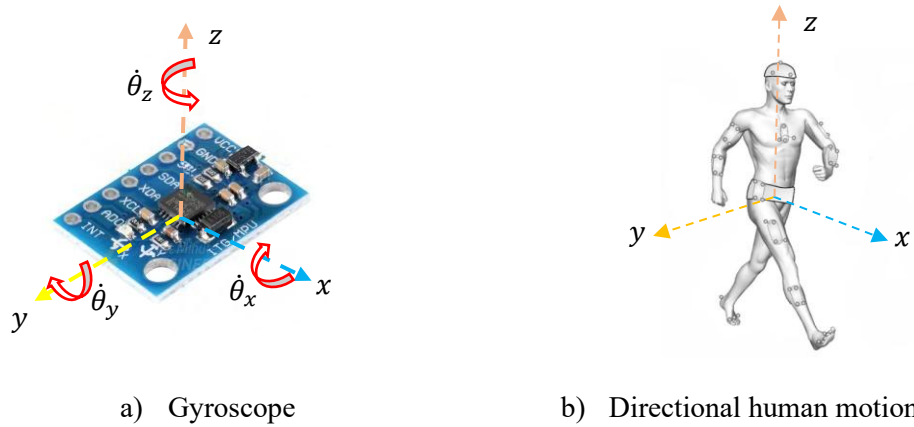
Figure 9:Gyroscope angular velocity directional measurements relative to the human walking

The gyroscope measurements (shown in Figure 9a) will capture the angular velocity of the lower limb segment where the IMU sensor is mounted. These measurements are oriented within the three-dimensional Cartesian plane of the individual, as illustrated in Figure 9b. The angular velocity is expressed in radians per second (rad/s) and is categorized into three rotational axes $\dot{\theta}_x$, $\dot{\theta}_y$, and $\dot{\theta}_z$ representing the angular

velocity about the x, y, and z directions, respectively. These measurements are important for analysing the gait cycle and understanding limb dynamics during movement.

1.2.4 Related Work

Recent studies have increasingly focused on analysing the gait cycle of individuals using wearable sensor systems that make use of Inertial Measurement Units (IMUs). The use of IMUs lies in their cost-effectiveness and versatility compared to traditional laboratory setups, which often constrain movement and create controlled environments that may not accurately reflect real-world conditions. This limitation makes them less applicable for monitoring human gait in real-world scenarios [18].

Most previous research has utilized either two or three IMU sensors placed on the lower limb. In studies employing two IMU sensors, they are typically positioned on the hip and shank. For example, the study by Mitchelle et al. for IMU Sensor to Segment Calibration [19] illustrates this setup. Conversely, studies that implement three IMU sensors add an extra sensor on the foot, as shown in the work of Tobias et al. on IMU to Segment and Orientation Alignment for Lower Body Using DL [20]. Figure 10a and Figure 10b provide visual representations of how the double and single IMU sensors are arranged on the lower limb segments for analysing the gait cycle

a) Two IMU system
b) Three IMU system
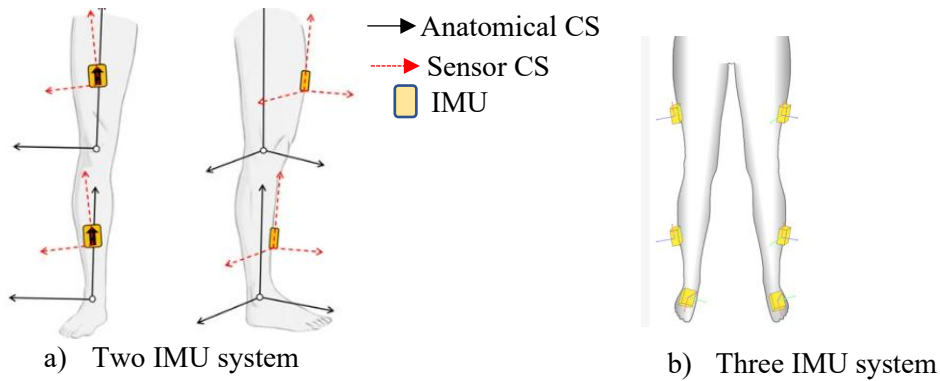
Figure 10:The 2 and 3 IMU sensor system configuration for gait cycle [19, 20]

1.2.5 Research objectives

The aims of this research are as follows:

1. Develop an Android application model that retrieves Inertial Measurement Unit (IMU) values of acceleration, angular velocity, and orientation, while the individual is in motion.
2. Analyse the gait cycle using the retrieved IMU data during movement.

2   METHODOLOGY

Approval for this research project was granted by the Human Research Ethics Committee (Non-Medical) due to the collection of data from a user. The ethics clearance number for this project is MIAEC 109/24W. One participant, a male in his 20s, contributed valuable insights for the research. The flow diagram below illustrates the methodology of this research, detailing the process from data collection to data processing. Further detail are provided in the following sections.

Figure 11:Flow diagram of the data collection to results

2.1   Development of Model for Data Collection

To access the IMU and GPS hardware values of the phone, an application model capable of retrieving real-time data from the sensors was developed. The application was created using the Android Studio Integrated Development Environment (IDE) version Ladybug | 2024.2.1 due to its features including an emulator for virtual testing during development without needing a physical device, and a layout editor for designing a user interface with built-in controls. The programming language used was Kotlin, as it allows for i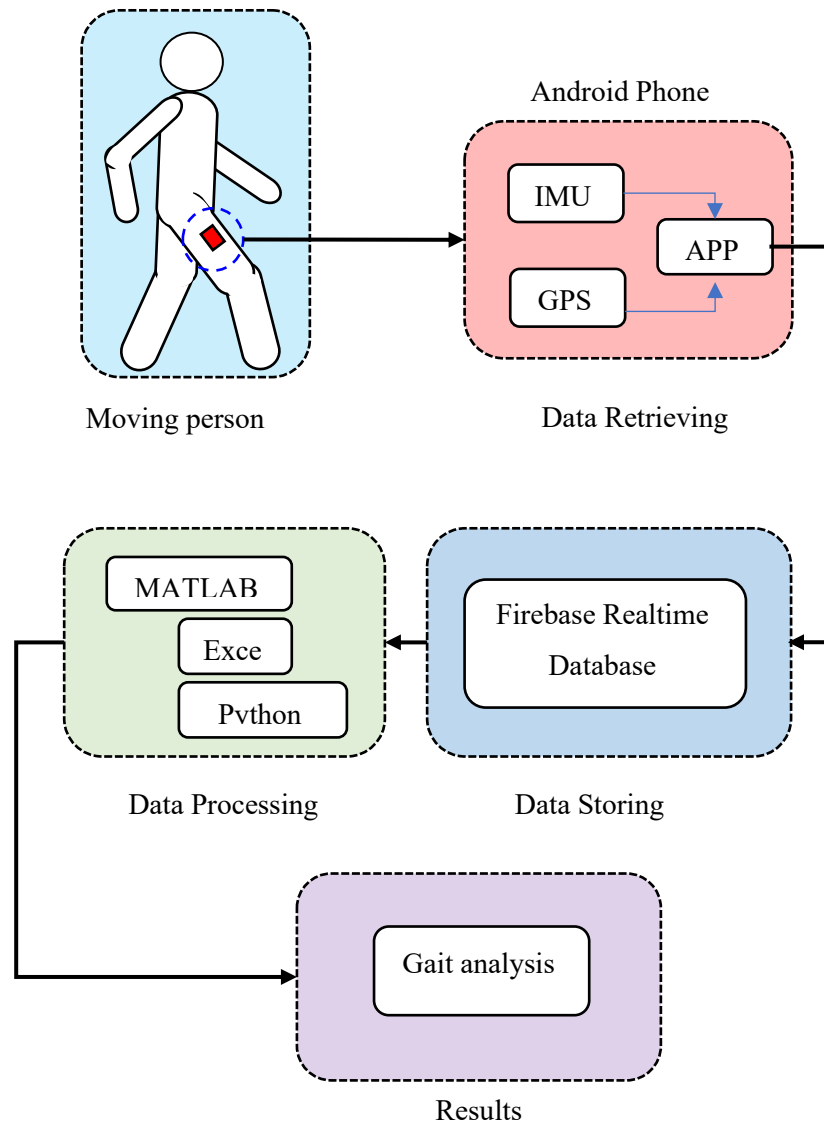mporting resources and libraries from Google services such as location that improve application performance for tracking.

The developed application model for data retrieving includes a user interface that displays sensor readings from the GPS and IMU hardware. The Figure 13 illustrates the layout of each section. The kinematics under IMU include acceleration, which records linear acceleration in the x, y, and z directions; angular velocity around the x, y, and z axes of the phone; and orientation, which captures the tilting of the phone based on pitch, roll, and yaw, as shown in Figure 12. Both types of kinematic data are updated using the predefined update rates of SENSOR_DELAY_FASTEST and SENSOR_DELAY_GAME, which provide the quickest updates reflecting the current state of motion.

For location tracking, GPS functionality was integrated into the user interface, enabling visualization of longitude and latitude for tracking the path taken, as well as calculating distance and average speed. For GPS to function, permission to access the device's location must be granted.

The user controls are designed to allow users to start and stop motion sensing on the device, with the ability to log motion data to a database at a specified sample rate, starting as low as 1 Hz. The database used is Firebase Realtime Database, which supports the storage of real-time data. Firebase was chosen for its provision of 1 GB of total storage and 10 GB/month of download capacity.
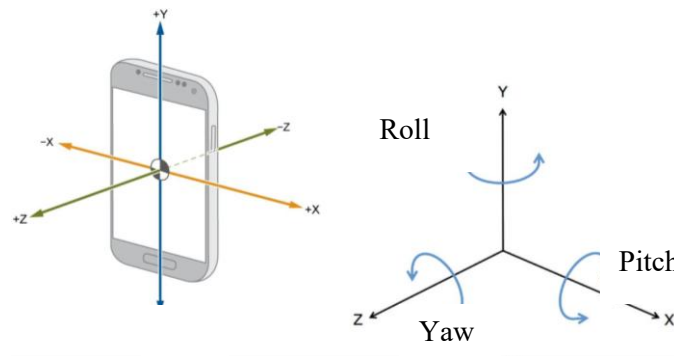
Figure 12: Mobile phone coordinate system [28]

The Figure 13 below illustrates the developed model for data collection designed to work on Android phones. The directions of acceleration, angular velocity, and orientation are based in the mobile phone coordinate presented in Figure 12 above.
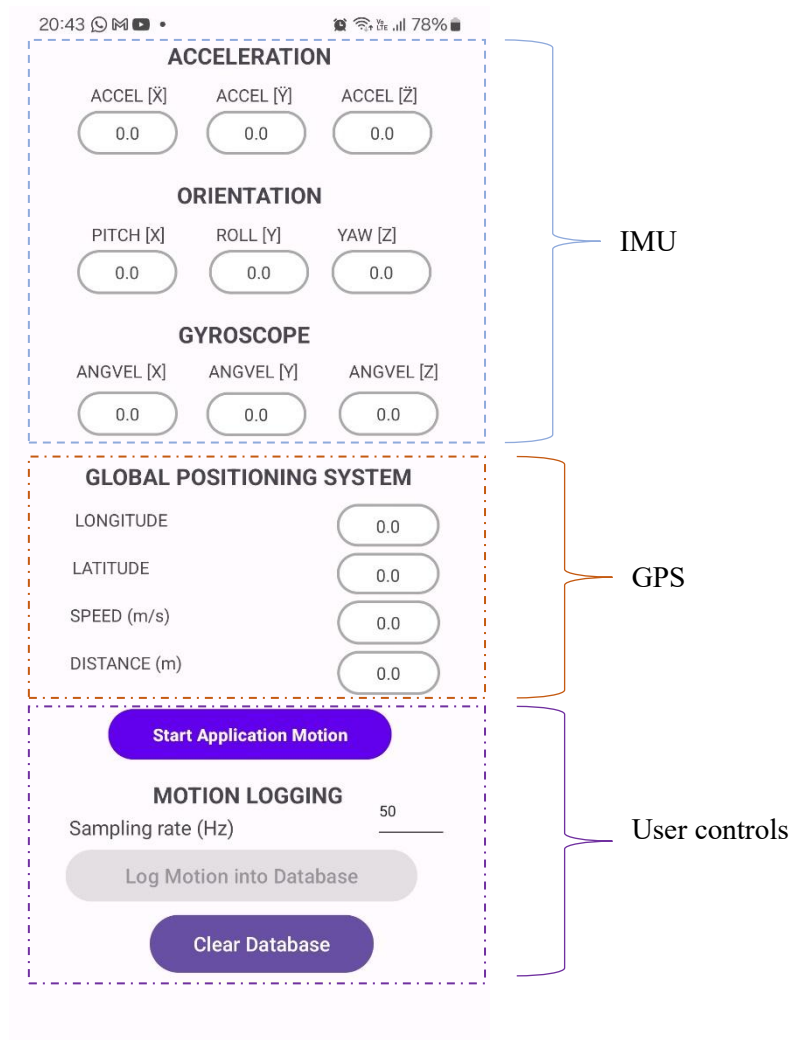
Figure 13: User Interface (UI) for data retrieving and collection model

To ensure the developed model code is functioning correctly, the virtual emulator and virtual sensors of the phone were configured for code validation. This process involved adjusting the sensor values to simulate various conditions and then monitoring the model's user interface in the emulator. This approach was to verify that the displayed values for acceleration, angular velocity, and orientation matched the expected outputs. Each adjustment was carefully tested to confirm that the code processes the sensor data accurately. The Figure 14 below shows the process of code functionality configuration

11

IDE Emulator virtual sensor and location	Mobile simulation on Emulator
a) Acceleration testing	
b) Orientation testing	
c) Angular acceleration testing	
d) GPS visualisation	d) Reflection of the visualisation of sensors reading being tested
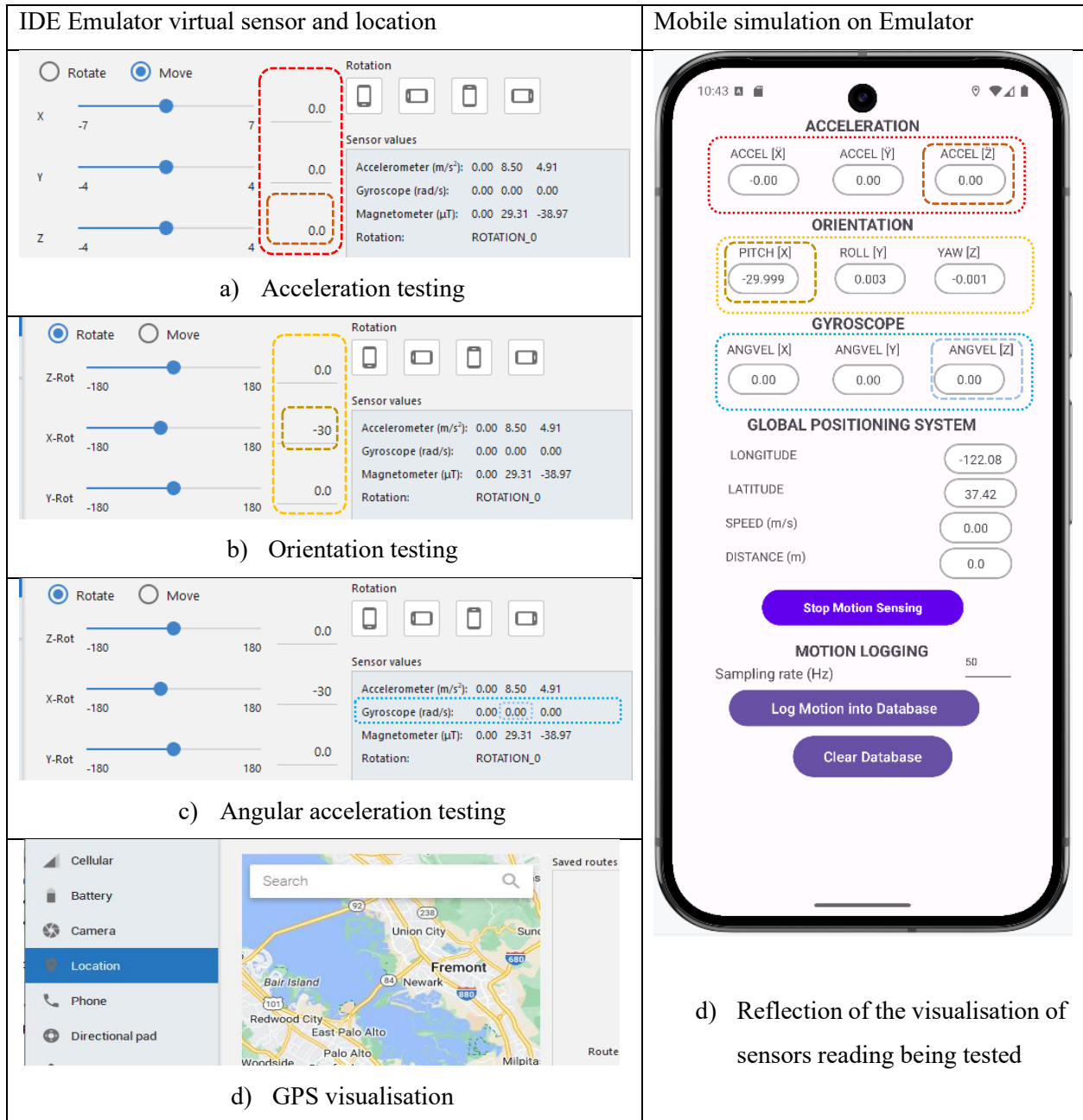
Figure 14:Verifying the functionality of the code

2.2 Data Collection Approach

The experiment was conducted using Huawei smartphone with the app installed. Motion data was recorded with the phone mounted on two different segments of the body: the shank, thigh, hand, and upper arm.. For each body segment, motion recordings were taken three times, differentiated by the type of movement: relaxed walking, fast walking, and jogging.

12

The motion data recorded from the Inertial Measurement Unit (IMU) included acceleration, orientation, and pitch, while GPS data provided longitude and latitude for motion tracking. For relaxed walking, a sampling rate of 25 Hz was set; for fast walking, the sampling rate increased to 50 Hz; and for jogging, a sampling rate of 75 Hz was employed. This increase in sampling rate from relaxed walking to jogging was implemented to accommodate the faster changes in motion occurring during these activities. As the speed of movement increases, the kinematic changes also require a higher sampling rate to accurately capture these variations, ensuring that the collected motion data reflects the true nature of the movements.

The same device was used throughout the data collection process, with a minimum distance travelled of 20 meters. This distance was chosen to ensure that the requested sampling rate did not exceed the limits of the database. Data collection was performed outside the building, as GPS tracking yields more accurate results outdoors compared to indoor settings.

3 DATA PROCESSING

This section presents the pre-processing of the data retrieved during the motion captured in the experiments.

3.1 Raw Data Cleaning and Prepossessing

The current raw data from the Inertial Measurement Unit (IMU) is displayed below Figure 15 in graphical format due to the large volume of sampled values. This dataset present only a relaxed walking scenario, with the phone placed in the left side pocket.
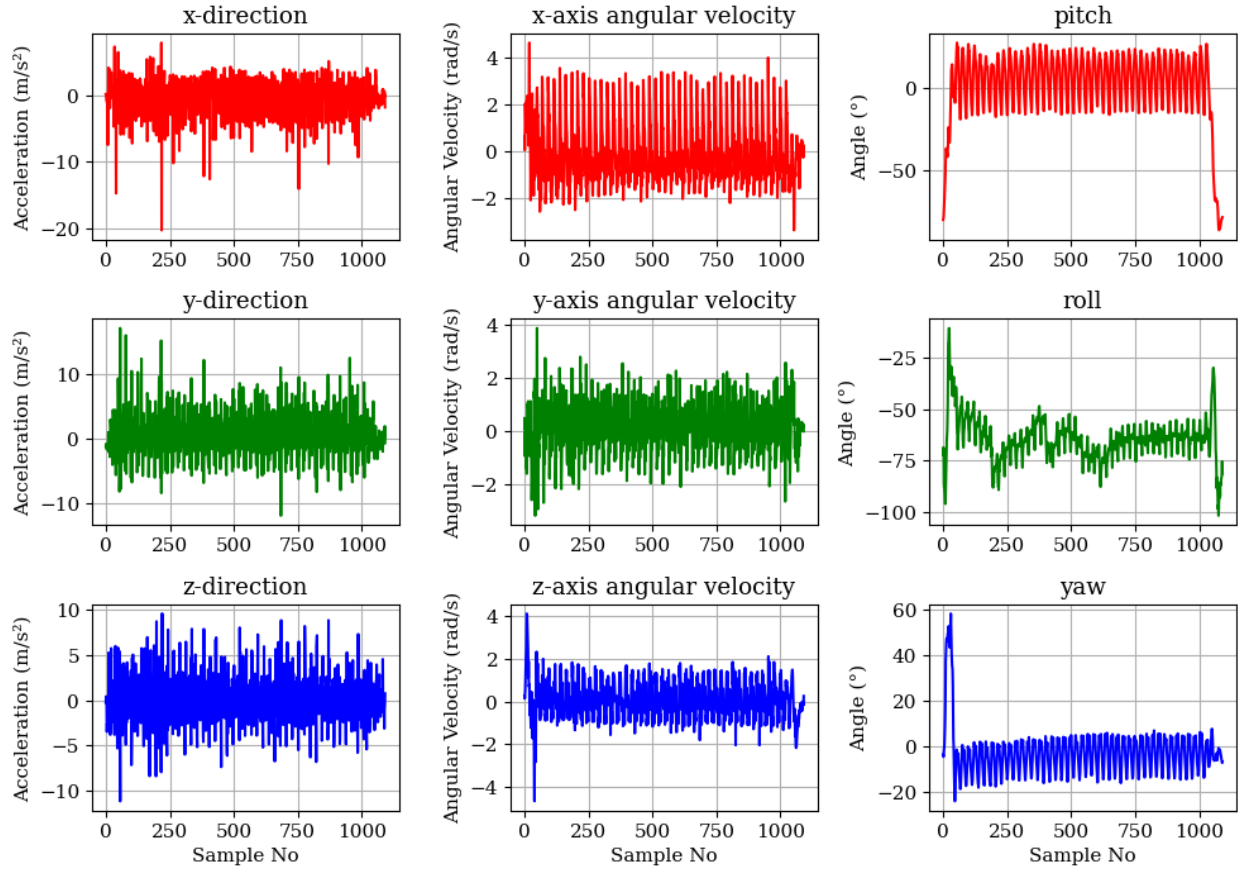
Figure 15:IMU graphical raw data for a relaxed walking with a phone on the left side pocket

The results in Figure 15 represent the acceleration in the x, y, and z directions, as well as the angular velocities about the x, y, and z axes. Additionally, the orientation data is included, indicating pitch, roll, and yaw angles.

The raw data from the GPS is presented in Figure 16 below, corresponding to the relaxed walking scenario with the phone in the left side pocket. This dataset includes latitude, longitude, total distance, and average speed

14

The distance between the two locations defined by longitude and latitude was determined using the Haversine formula, a mathematical approach for measuring the distance between two points [21]. The formula calculates the distance along the shortest path between the points, which are specified by their latitude and longitude coordinates.

$$distance = 2R \times arcsin\left(\sqrt{sin^2\left(\frac{\varphi_1 - \varphi_2}{2}\right) + \cos(\varphi_1)\cos(\varphi_2) + sin^2\left(\frac{\lambda_1 - \lambda_2}{2}\right)}\right)$$

where R is the Earth's radius (6,371 km), $\varphi_1 - \varphi_2$ are the latitudes of the two locations (in radians), and $\lambda_1 - \lambda_2$ are the longitudes of the two locations (in radians).

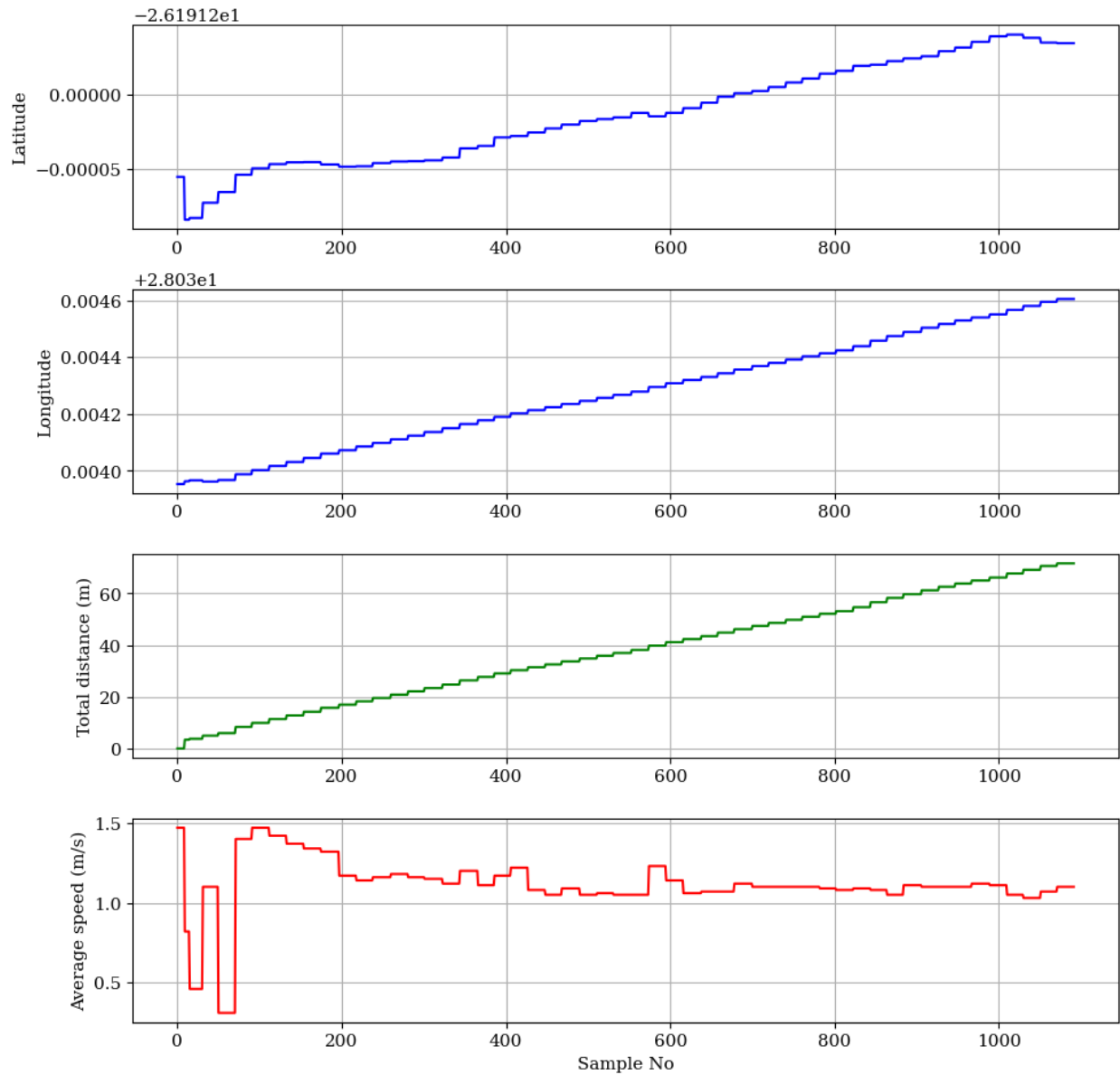Figure 16: Processing of GPS data to get the distance and average speed

15

During pre-processing, the first 75 and last 75 sampled values are removed for the relaxed walking scenario. These values represent the initial and final 3 seconds of data collection, which do not accurately capture true motion, as they include the moments of placing the phone in the pocket and removing it.

For the fast-walking scenario, the first and last 150 samples are discarded, reflecting the average sampling rate used during this activity. In the case of jogging, the first and last 225 samples are removed, as this data is collected at a higher sampling rate. This method ensures that the processed data accurately reflects the actual motion for each activity.

3.2   Verification and Validation of the data

To validate the IMU, the GPS was used. Before using the GPS for validation, the recorded latitude and longitude obtained from the model, which defined the tracking of the person, were traced on Google Maps. This was done to determine whether the coordinates accurately represented the actual path travelled during data collection. The latitude and longitude data from the model for each experiment are shown in the figure below for path tracking.
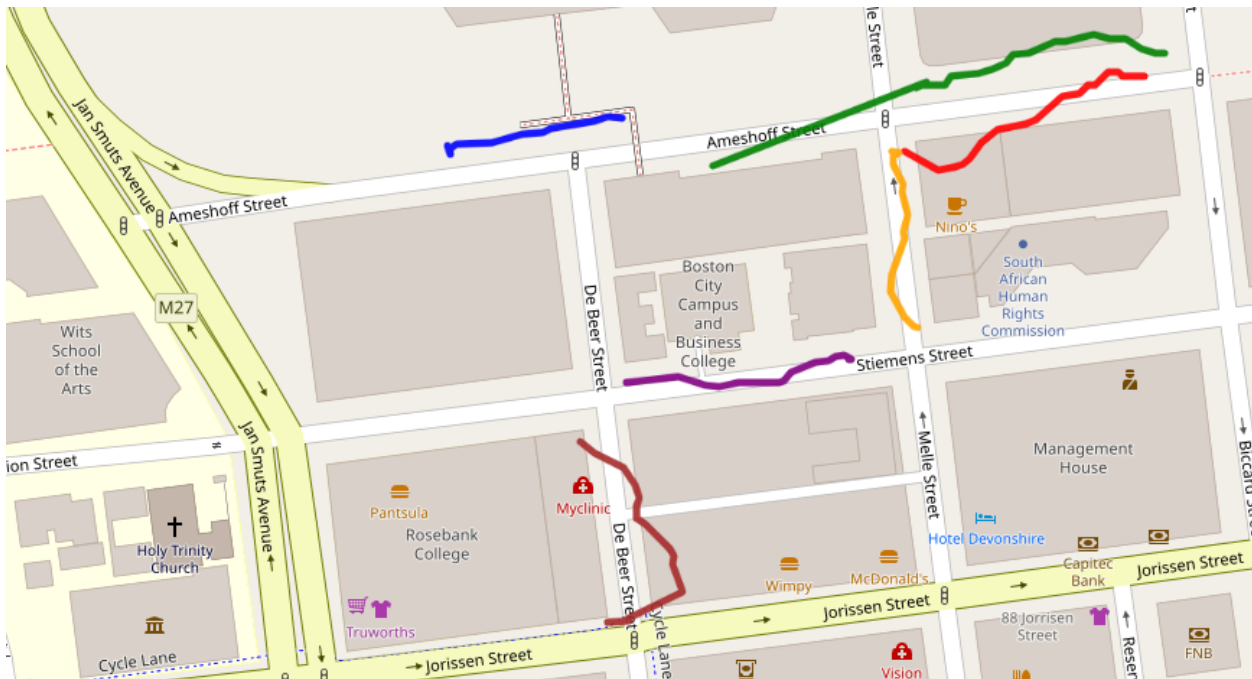

Figure 17: Traced path during the data collection

In both cases, the latitude accurately represented the actual path taken during the motion. The coordinates could be used to validate the sensor, as they effectively traced the actual walking path, as illustrated in the Figure 17 above.

16

To analyse the data collected from the Inertial Measurement Unit (IMU), which includes acceleration $\ddot{x}(t)$ measurements in three-dimensional space, integration techniques from calculus is used. The recorded acceleration can be integrated to determine the velocity $\dot{x}(t)$ and position displacement $x(t)$ over time, using the following equations.

Velocity calculation:

$$\dot{x}(t) = \int \ddot{x}(t) + \dot{x}_0\,(t_0)$$

where $\dot{x}_0$ is the initial velocity at time t_0

Position calculation:

$$x(t) = \int \dot{x}(t) + x_0(t_0)$$

where x_0 is the initial; position at time t_0

Because the acceleration data collected from the IMU is not continuous and consists of discrete samples taken at various points during motion, numerical integration methods is employed to accurately estimate velocity and position. The cumulative trapezoidal rule is used for numerical integration to handle the discrete nature of the data. The numerical integration equations used are detailed below

Numerical Integration

Velocity approximation:

$$\dot{x}(t_i) = \dot{x}(t_{i-1}) + \frac{t_i - t_{i-1}}{2}\left(\ddot{x}(t_{i-1}) + \ddot{x}(t_i)\right)$$

where $\dot{x}(t_i)$ is the estimated velocity at time t_i

Position approximation

$$x(t_i) = \dot{x}(t_{i-1}) + \frac{t_i - t_{i-1}}{2}\left(\dot{x}(t_{i-1}) + \dot{x}(t_i)\right)$$

where $x(t_i)$ is the estimated velocity at time t_i

By applying these numerical integration techniques, both velocity and position can be effectively estimated based on the discrete acceleration data collected from the IMU
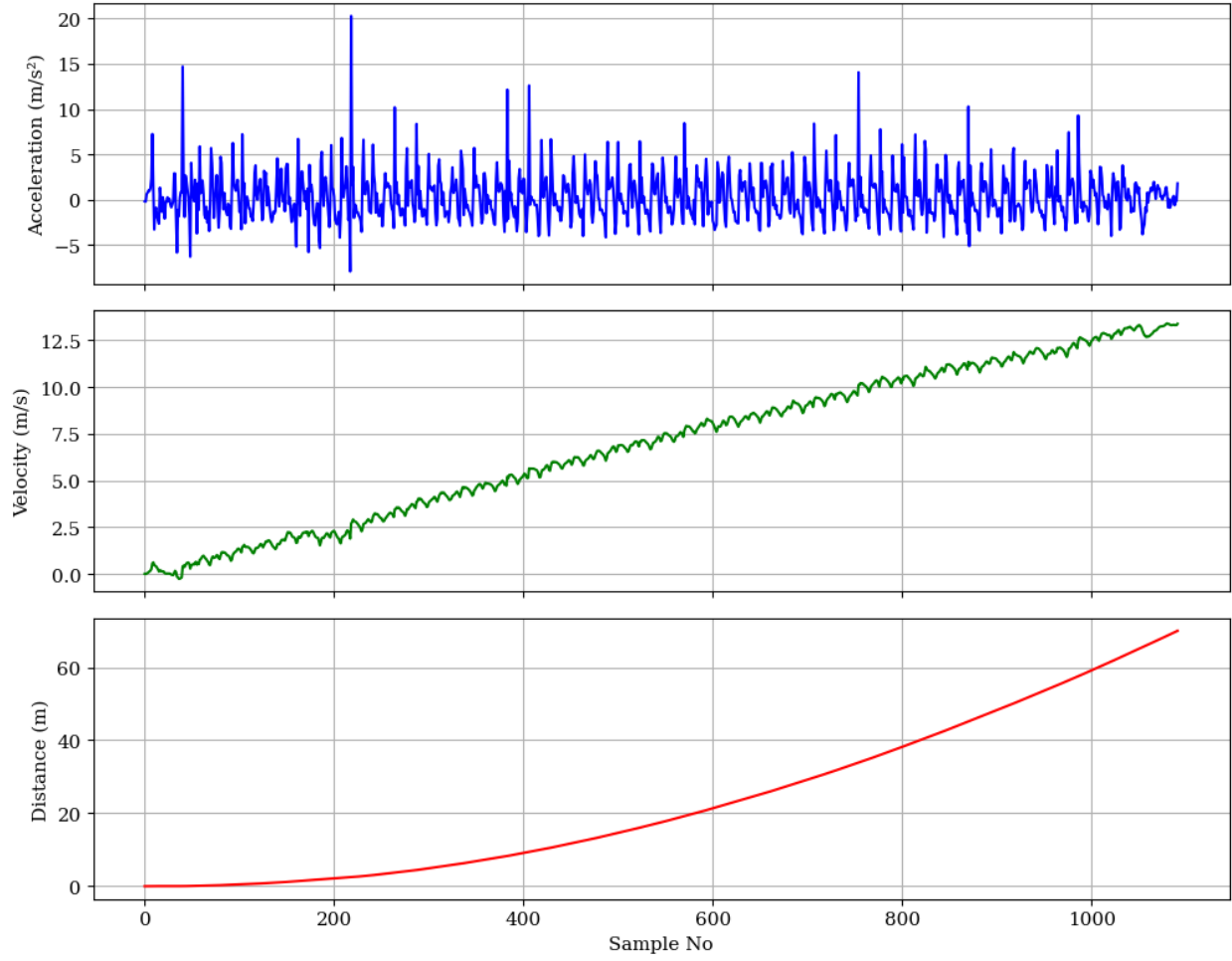
Figure 18:Using IMU to approximate the distance

a) GPS Total distance   b) IMU Total distance
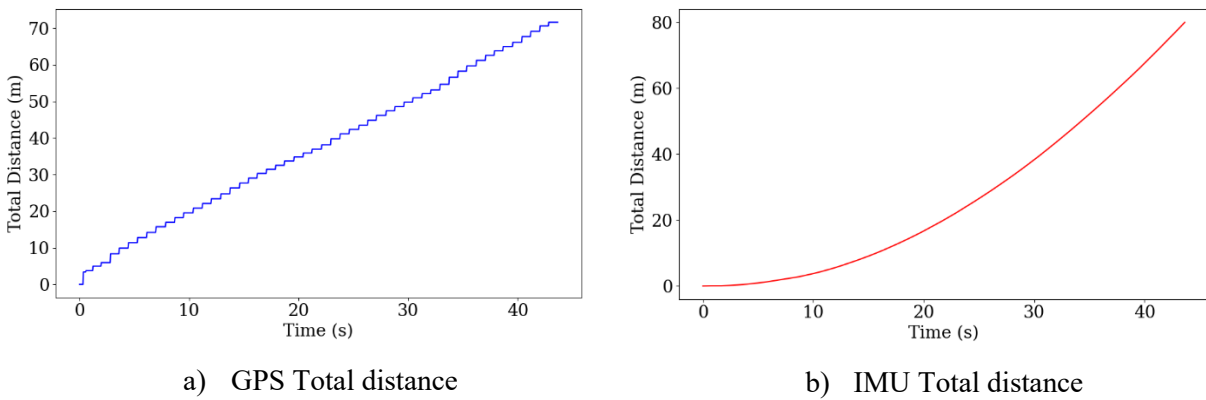
Figure 19:IMU and GPS total distance validation

The comparison between GPS and IMU total distance Figure 19 shows that although the GPS output increases linearly while the IMU follows a nonlinear trend, both methods yield comparable total distances over the same time duration

4 RESULTS A ND DISCUSSION

4.1 Gait Identification from IMU

This section presents an analysis of the gait cycle phases derived from data collected during motion. The focus is on the mapping of the Stance and Swing phases, as described in the literature review. The analysis includes three types of gaits: relaxed walking, fast walking, and jogging.

4.1.1 Relaxed walking gait cycle

For the motion of the user when relaxed walking with the phone inside the left pocket, after being processed were mapped with the gait cycle as shown below in Figure 20.

Figure 20:Mapping of relaxed walking motion to gate cycle

In the case of relaxed walking, where the user carried a phone in the left pocket, the processed data was used to map the gait cycle, as depicted in Figure 20.

Stance phase dynamics

From the analysis, gait identification was primarily based on three key parameters: acceleration in the x-direction, angular velocity around the y-axis, and the tilt angle of yaw. Each of these parameters plays a critical role in understanding the user's motion:
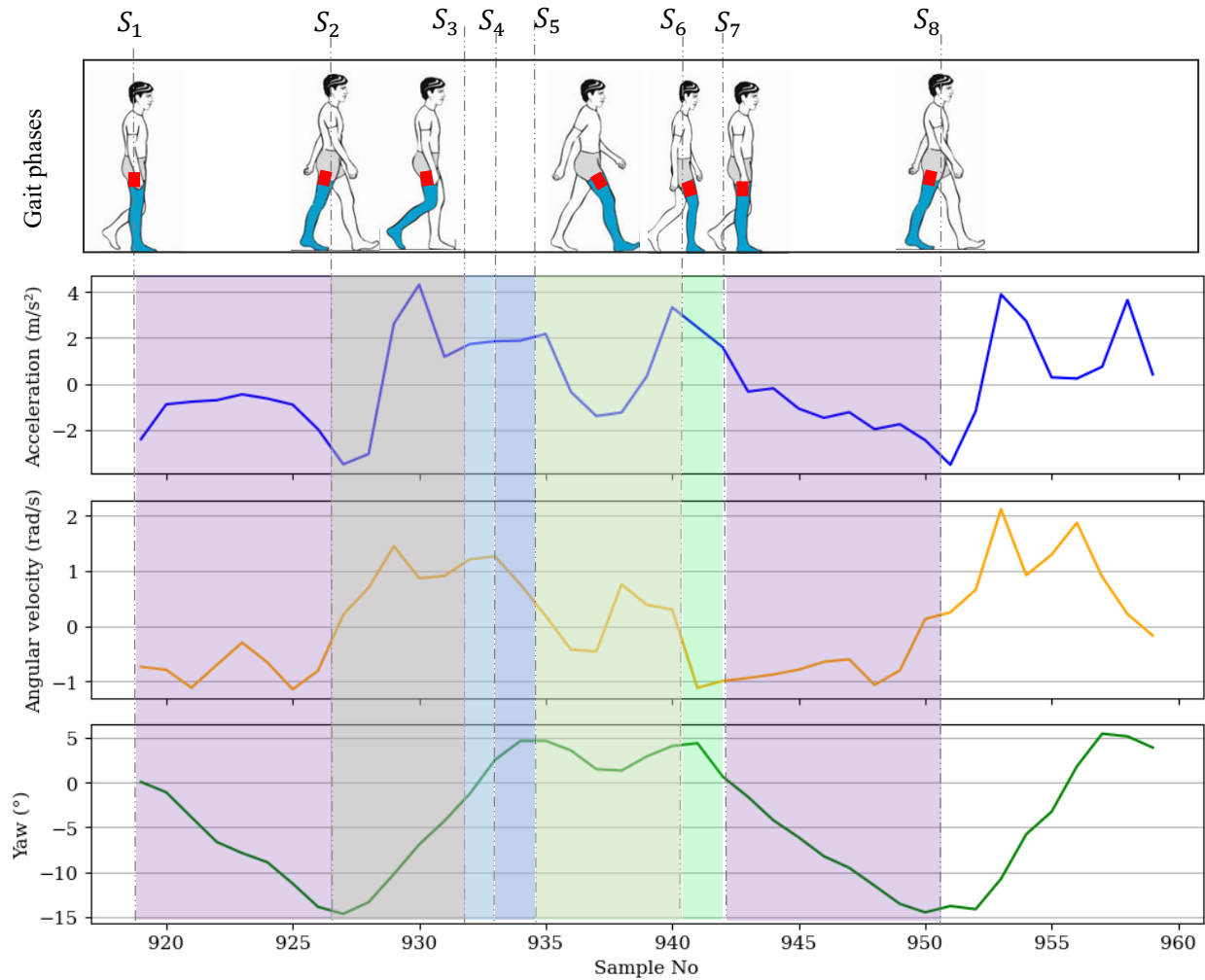
- **Mid-stance (S1):** This phase is defined as the position where the leg is straight forward and perpendicular to the ground, with the yaw angle at zero. This position indicates optimal stability and weight distribution.

- **Transition to terminal stance (S1 → S2):** As the user transitions from mid-stance to terminal stance, the angle of the leg reaches a minimum (approximately -15°). This change occurs because the leg extends backward, preparing to propel the user forward. The observed fluctuations in acceleration and angular velocity during this transition underscore the variable nature of walking, as the user's velocity is not constant, evidenced by changes in average speed.

- **Terminal stance (S2):** In this phase, the leg reaches its furthest backward position, resulting in minimal acceleration. This is a critical moment, as it indicates that the user is preparing to transition into the next phase of the gait cycle.

Pre-Swing Phase Dynamics

- **Pre-swing (S2 → S1):** Here, the leg begins to accelerate forward from the terminal stance. This increase in acceleration and yaw angle reflects the leg's movement as it prepares to initiate forward propulsion. The transition to this phase is marked by increasing thigh angle as the leg moves forward.

- **Toe-off and mid-swing (S3 → S4 and S4 → S5):** The phases of toe-off and mid-swing indicate the leg's maximum forward motion. Although the acceleration, angular velocity, and thigh orientation are estimated, the transitions can be approximated based on the data. The peak thigh angle at S5 signifies that the leg is fully extended forward, ready to strike the ground in the next cycle.

Swing phase dynamics

- **Terminal swing (S5):** Following the mid-swing, the leg prepares for ground contact. A sudden deceleration is noted here, confirming that the leg's movement must adjust rapidly in anticipation of the heel strike. This aligns with the gait cycle's expectation that the leg will decelerate in preparation for a stable ground contact.

- **Loading response (S6):** Upon ground contact, the leg enters a loading phase. The angle decreases, and acceleration approaches zero as the leg absorbs the impact. This phase confirms the stabilization of the body weight onto the stance leg.
- **Mid stance (S7):** After the loading phase, the leg returns to mid-stance, completing the gait cycle. This cyclical process continues during relaxed walking, illustrating the repetitive nature of human locomotion.

The analysis aligns well with the established understanding of the gait cycle, as outlined in the literature review. A normal gait cycle begins and ends with a heel strike, marking the transition from the load response phase to double support, where both feet contact the ground. The mid-stance phase, characterized by the opposite leg entering the swing phase, is essential for forward progression.

4.1.2   Fast walking gait cycle

During fast walking, the retrieved data mapped with the gait cycle is illustrated in Figure 21. The analysis of fast walking relies on three key parameters: acceleration in the x-direction, angular velocity about the z-axis, and orientation indicated by the yaw angle.
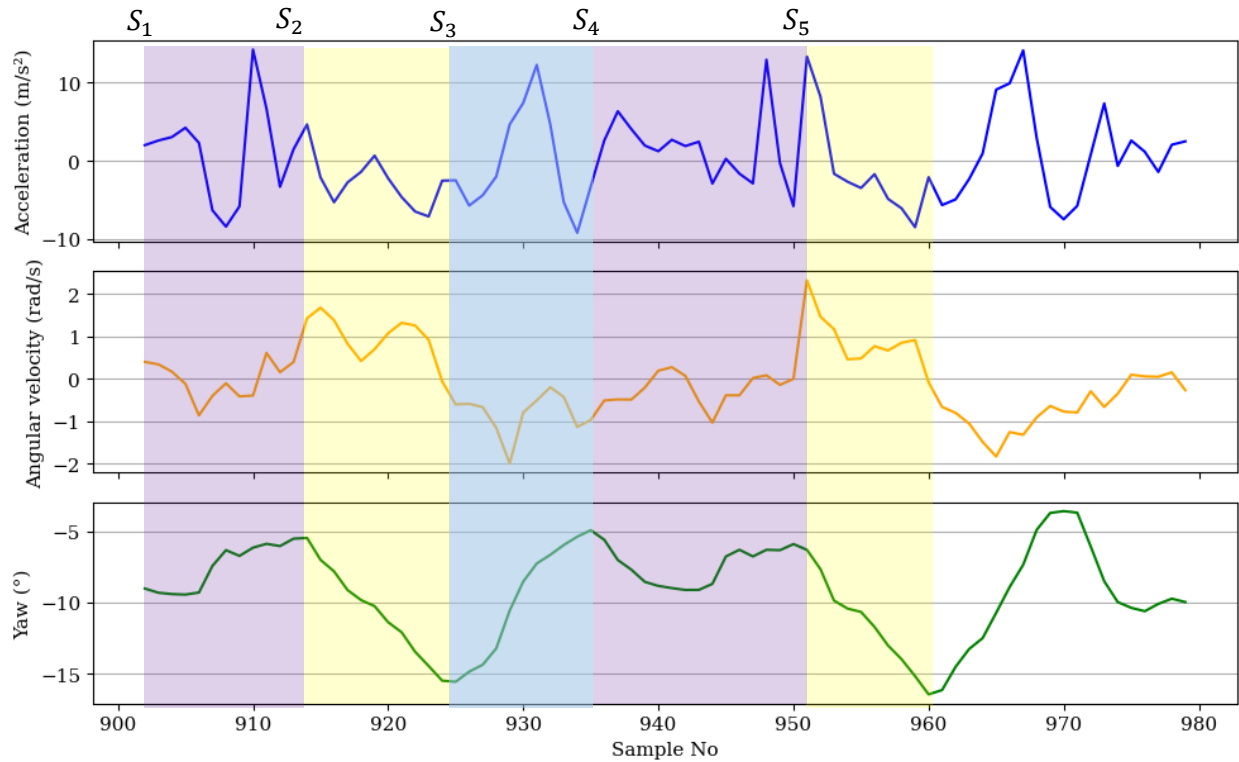

Figure 21:Mapping gait cycle for fast walking with phone inside left pocket

For this analysis, S1 is designated as the reference point. S2 represents the maximum angle, approximately -5°, which corresponds to the terminal swing phase of the gait cycle. This maximum angle is critical as it indicates the transition into the next phase.

- **Heel Strike and Loading Response:** At S2, the heel strike occurs as the left leg makes contact with the ground, exhibiting an acceleration of approximately 5 m/s². This sudden impact is crucial for understanding the dynamics of the gait cycle. Following the heel strike, a notable change in angular velocity is observed, accompanied by fluctuations. These changes can be attributed to the phone not being securely placed in the pocket. The impact of the heel striking the ground, combined with inertia, causes the phone to shift until it settles back into the pocket.

- **Transitioning segment S2 to S3**: the loading response takes place at this segment. This phase is characterized by the leg absorbing the impact of the ground strike, which is essential for maintaining stability and preparing for the next phase of the gait cycle.

- **Transition to Terminal Stance (S3):** After the loading response, the leg begins to return to a stance position, ultimately reaching terminal stance, denoted as S3. At this point, the angle is at its lowest, approximately -17°. This position is significant as it represents a moment of maximum stability, where the body weight is fully supported by the stance leg.

- **Forward Swing and Maximum Acceleration: Following** the terminal stance, the leg transitions into the swing phase, where it begins to move forward. As the angle increases during this forward motion, the acceleration reaches a peak of approximately 12 m/s². This acceleration signifies the force exerted as the leg propels the body forward, illustrating the dynamic nature of fast walking.

4.2   Arm Swing Cycle Identification from IMU

This section presents the mapping of the arm motion as it correlates to the phases of the gait cycle, as detailed in the literature review, with the corresponding figure illustrating the different swing phases of the arm. The phases are for relaxed walking, fast walking, and jogging with a mobile held by left hand.

4.2.1   Relaxed walking arm swing cycle

The motion of relaxed walking with the phone held in the left hand is shown in the figure below, where the movement is divided into distinct segments. The stick figure, though not drawn to scale, represents the

arm swing motion at various points in the gait cycle. These segments highlight the coordination between the arm's forward and backward swings, which correspond to the leg movements, as detailed in the gait cycle analysis. The figure illustrates how the arm's motion varies throughout the cycle, contributing to overall balance and energy efficiency during walking. Each segment captures a specific phase of the arm swing.
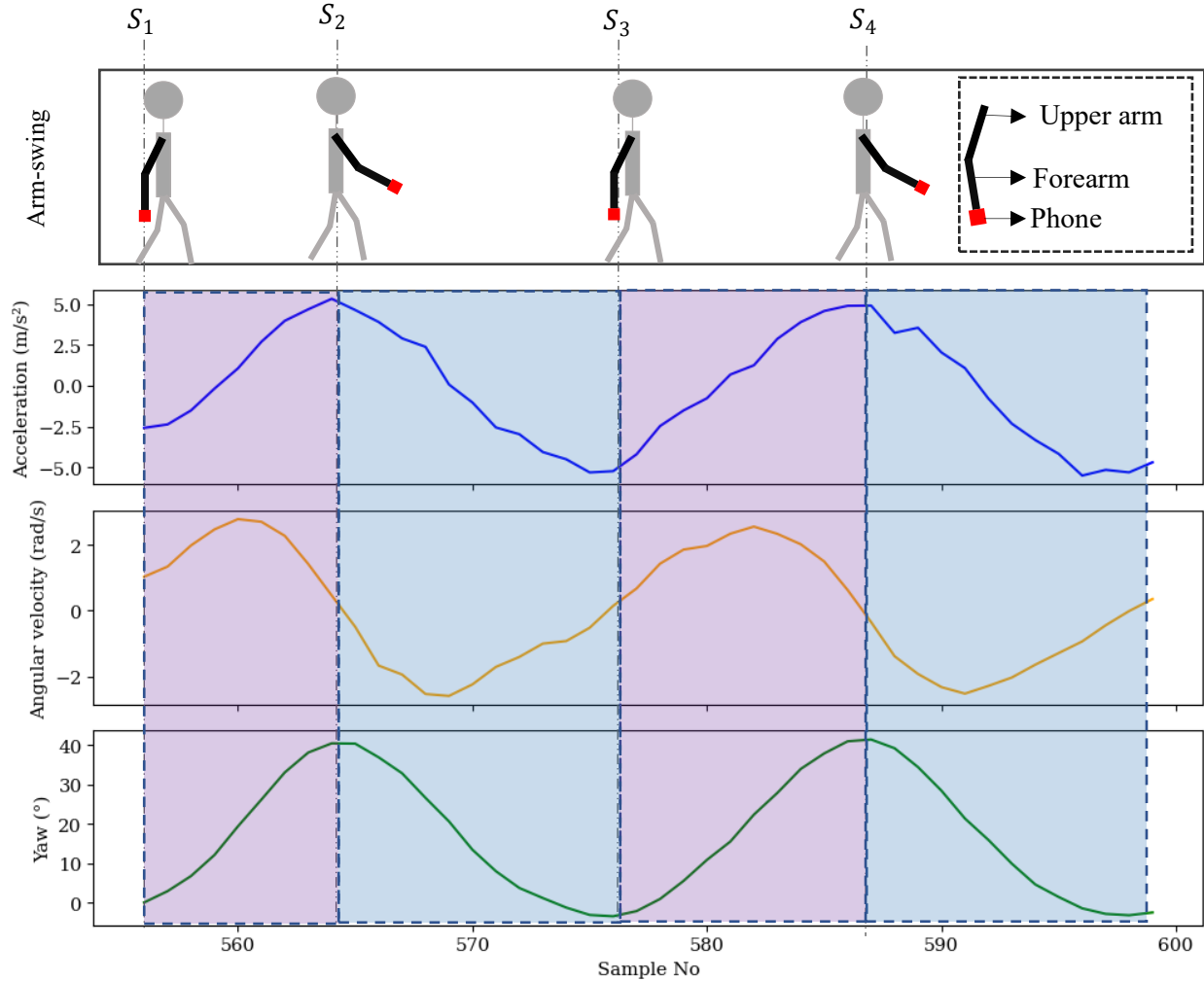
Figure 22:Mapping of arm swing cycle to the retrieved data from IMU

Mapping of the Arm Swing

The cycle of the arm swing is mapped starting from the mid-swing forward direction (denoted by position S1). In this position:

- **S1 (Mid-Swing Forward):** The arm is in the mid-swing phase, where the yaw angle is 0°, and the arm is parallel to the body. At this point, the arm experiences its minimum acceleration, as it is neither accelerating forward nor backward.

- **S1 to S2 (Forward Swing and Acceleration):** As the arm continues to swing forward from S1 to S2, the angle of the arm increases, and it accelerates in the forward direction. The arm reaches its maximum acceleration of 5 m/s² during this phase. At S2, the arm reaches its maximum forward position, with the angular velocity being 0 rad/s, as it momentarily stops before changing direction. The arm's angle reaches a maximum of approximately 38°.

- **S2 to S3 (Backward swing and deceleration):** After S2, the arm begins to swing backward. The swing direction reverses, and the arm accelerates in the opposing direction. As the arm reaches the mid-swing backward phase (denoted by S3), it experiences minimum acceleration once again. The arm's orientation is now at 0°, similar to its initial position in S1. This marks the completion of one full cycle, which then repeats.

4.2.2 Fast walking arm swing cycle

The mapping results for fast walking with the phone held in the left hand are shown in the figure below. This mapping illustrates the differences in the arm swing dynamics compared to relaxed walking, including variations in acceleration, swing angles, and angular velocity.
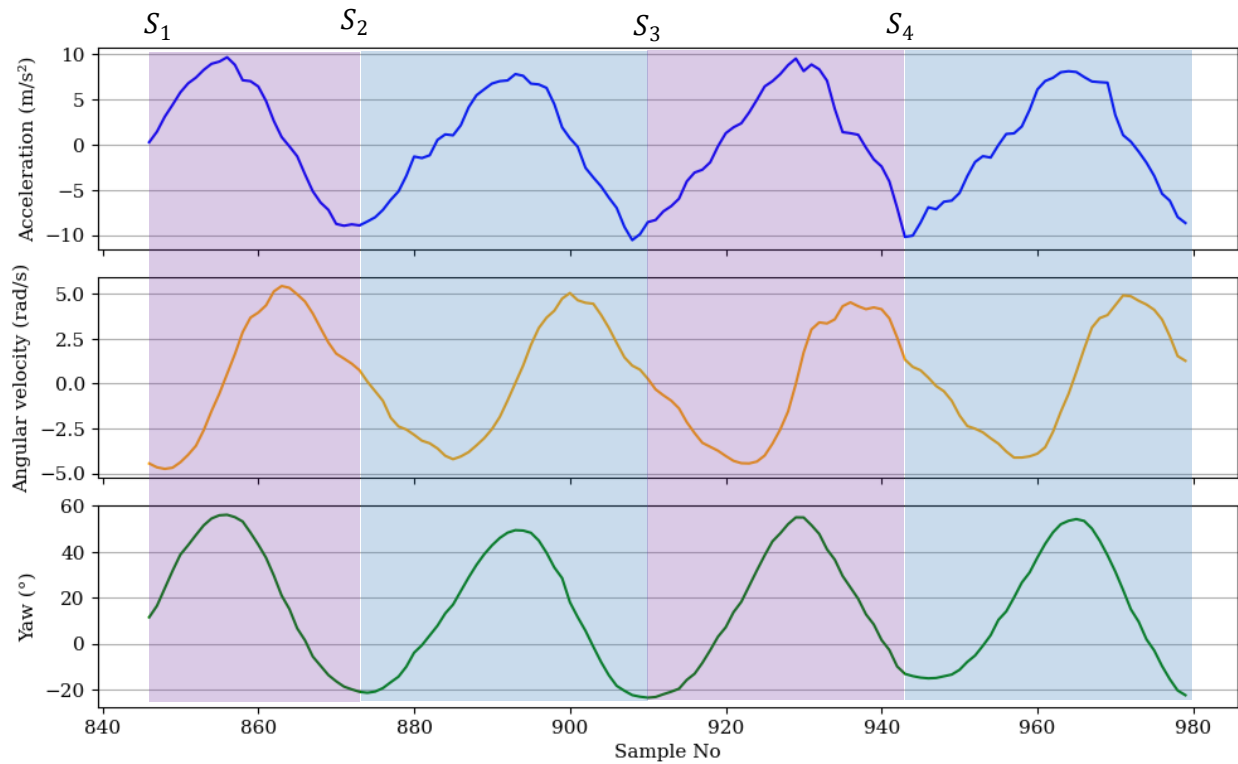

Figure 23:Mapping of fast walking arm swing cycle

During fast walking, the arm swing pattern follows a similar cycle to relaxed walking, but with notable differences in terms of cycle time, acceleration, and swing angles. While the basic coordination of arm and leg movements remains the same, the parameters differ due to the increased speed of walking.

24

- **Maximum and minimum acceleration:** In fast walking, the arm experiences a much higher acceleration, reaching a maximum of 10 m/s² and a minimum of -10 m/s², compared to the lower accelerations observed during relaxed walking.
- **Swing angles:** The arm's swing amplitude is greater, with maximum and minimum swing angles of approximately 58° and -20°, respectively, reflecting the increased range of motion in fast walking.
- **Angular velocity:** The arm's angular velocity also increases, reaching a maximum of 5 rad/s and a minimum of -5 rad/s, indicating the faster motion and quicker transitions between forward and backward swings.

These differences reflect the increased intensity and speed of the movement in fast walking, which leads to higher accelerations, greater angular velocities, and a broader range of arm motion compared to the relaxed walking cycle

4.3   Overall Identified Gait Cycle statics

The overall calculated gaits for relaxed, fast, and jogging motions, with the mobile phone placed in both the pocket and the hand, are presented in Table 1 and Table 2.

Table 1:Calculated gaits for pocket placement of the mobile phone

Acceleration (m/s^2)				
	Mean	Max	Min	Std
Relaxed	-0,31695	7,93916	-20,2818	2,70778
Fast	-0,09044	8,86816	-19,0051	3,14046
Jogging	0,37244	10,2242	-26,9618	5,12404
Angular Velocity (rad/s)				
	Mean	Max	Min	Std
Relaxed	0,03823	2,79464	-2,18652	0,85096
Fast	0,01285	6,64679	-3,52965	1,43217
Jogging	0,07408	6,63614	-5,70925	1,9805
Orientation [Yaw] (degree)				
	Mean	Max	Min	Std
Relaxed	-3,91995	6,9226	-17,6953	6,37232
Fast	-3,2336	66,0971	-13,9558	9,24381
Jogging	-9,33518	-0,67476	-20,3876	3,81914

Table 2:Calculated gaits for hand placement of the mobile phone

Acceleration (m/s^2)			
	Mean	Max	Min	Std
Relaxed	0,067	7,0317	-6,448	3,8087
Fast	-0,034	13,211	-12,66	6,4649
Jogging	3,3617	35,945	-28,08	14,6
Angular Velocity (rad/s)			
	Mean	Max	Min	Std
Relaxed	-0,016	2,7106	-1,534	0,6168
Fast	-0,005	2,6347	-3,63	0,766
Jogging	-0,076	4,417	-5,721	1,7179
Orientation [Yaw] (degree)			
	Mean	Max	Min	Std
Relaxed	13,683	45,25	-15,8	16,805
Fast	13,039	74,987	-34,28	29,038
Jogging	44,586	80,673	-12,3	23,256

4.3.1 Rate of the forward movement

Acceleration along the x-axis provides an important measure of the forward motion of the body during walking. The results from the different motion conditions relaxed, fast, and jogging showed clear distinctions in both the magnitude and variability of acceleration.

Phone inside left side pocket for relaxed, fast, and jogging

For a relaxed walk, the mean acceleration was -0.3169m/s^2 , indicating a slight deceleration in the forward direction during relaxed motion with a standard deviation of 2.7078 m/s^2 suggests that the motion was more consistent with slow walking. The maximum acceleration 7.9392 m/s^2 and minimum -20.2818 m/s^2 For relaxed walking, both the maximum and minimum acceleration values are high. These accelerations can be traced back to the path taken, as it was not smooth. In some areas, there were steep discontinuities in the otherwise even path, which likely led to changes in acceleration.

During the fast-walking motion, the mean acceleration increased slightly to -0.0904 m/s^2, and the standard deviation increased to 3.1405 m/s^2, indicating more variation in the forward motion. This is expected as

walking faster involves greater fluctuations in acceleration due to changes in pace. During jogging motion, a significant change occurred during this motion with a mean acceleration of $0.3724\ m/s^2$, indicating a positive forward motion. The large standard deviation of $5.1240\ m/s^2$ reflects the irregular nature of jogging, which involves higher forces and larger fluctuations in acceleration as the body moves faster and with more forceful steps. The maximum acceleration of $10.2242\ m/s^2$ represent the consistent with the increased intensity of jogging.

Phone held by left Hand

The mean acceleration of $0.0670\ m/s^2$ for relaxed walking with the phone held in hand was positive, suggesting a more stable movement compared to the pocket condition. The standard deviation (3.8087) was larger, reflecting slightly more variability in the hand-held condition and for fast walking, the standard deviation increased to (6.4649), which is consistent with the more pronounced fluctuations observed when walking at a faster pace. The maximum acceleration of $13.2112\ m/s^2$ reached its highest value in the hand condition, indicating more dynamic movement compared to the pocket condition.

During jogging, the acceleration was highly variable, with a mean of $3.3617\ m/s^2$ and a large standard deviation of 14.5998, reflecting the intense motion of jogging. The maximum acceleration $35.9450\ m/s^2$ was much higher than any other condition, highlighting the significant increase in forward movement during jogging when the phone is held in the hand

4.3.2 Orientation of body segment

Yaw in this research project was describing the angular displacement of the device relative to the x-axis, indicating the angle of the thigh during different phases of walking. A minimum yaw corresponds to the terminal stance phase, where the leg is fully extended whereas maximum yaw indicates the terminal swing phase, just before the heel strike, where the leg is in the swing phase.

Phone inside a pocket

During the relax motion, the mean yaw was -3.92°, indicating that during relaxed walking, the thigh was positioned closer to the terminal stance phase. The standard deviation of 6.37° suggests that there was some variability in thigh rotation and for a fast walk, the mean yaw decreased slightly to -3.23°, indicating that the device remained in a position close to the terminal stance phase during fast walking, with the thigh in a similar orientation. The smaller standard deviation of 3.82° suggests that the rotation of the thigh was more stable during faster walking, with less variability in the leg's movement and for jogging, the yaw during jogging showed larger fluctuations, with a mean value of -3.23° and a standard deviation of 9.24°.

27

This suggests that there was significant rotational movement of the thigh due to the increased dynamics of jogging, considering the higher force and speed during this activity.

Phone held by left hand

The mean yaw for the hand-held condition during relaxed walking was 13.68°, indicating a shift toward the terminal swing phase of the leg. This suggests that during relaxed walking with the phone held in the hand, the leg was positioned just before the heel strike, with outward rotation of the thigh. The high standard deviation (16.81°) indicates substantial variation in the thigh's orientation, likely due to more noticeable body rotation and posture changes. During fast walk, the mean yaw decreased slightly to 13.04°, and the standard deviation of 29.04° was still quite large compared to the relaxed walking condition. This suggests that while the thigh's rotation remained in the terminal swing phase, the phone's orientation was still quite variable, reflecting the faster movements during fast walking.

The yaw showed the highest variation during jogging, with a mean of 44.59° and a standard deviation of 23.26°. This large variation indicates that during jogging, the phone experienced significant rotation, as the thigh's orientation shifted between the terminal swing and heel strike phases with increased dynamics and force.

5 CONCLUSIONS AND RECOMMENDATIONS

This study demonstrates the feasibility and effectiveness of using a single Inertial Measurement Unit (IMU) for gait cycle analysis in real-world settings, facilitated by a custom Android application. The project successfully identified distinct gait phases (stance and swing) across various movement types, including relaxed walking, fast walking, and jogging. Results show that a single IMU system, positioned at various points on the body, can capture essential gait characteristics such as acceleration, angular velocity, and orientation, achieving an analysis quality comparable to multi-sensor setups. This portable approach presents a practical and non-intrusive solution for gait analysis, with potential applications in healthcare for patient mobility monitoring, in security for biometric identification, and in fitness for tracking personal performance.

Recommendations

To build on these findings, future work should consider expanding data collection by incorporating a more diverse participant group, including individuals of varying age groups, body types, and gait abnormalities, to improve model robustness and generalizability. Enhancing the Android application's interface and adding automated data cleaning features would improve usability and broaden accessibility. Implementing real-time gait analysis and feedback functionalities could provide immediate insights, which would be especially valuable in rehabilitation and fitness tracking contexts

REFERENCES

[1] S. Dimple, B. Sourabh and P. Chandra , "A comprehensive survey on gait analysis: History,," *Artificial Intelligence in Medicine,* vol. 129, p. 102341, 2022.

[2] Saboor, Abdul and Kask, Triin and Kuusik, Alar and Alam, Muhammad and Le Moullec, Yannick and Niazi, Imran and Zoha, Ahmed and Ahmad and Rizwan, "Latest Research Trends in Gait Analysis Using Wearable Sensors and Machine Learning: A Systematic Review}," *IEEE Access,* vol. 8, 09 2020.

[3] Chen, Xin and Weng, Jian and Lu, Wei and Xu and Jiaming, "Multi-Gait Recognition Based on Attribute Discovery," *IEEE Transactions on Pattern Analysis and Machine Intelligence,* vol. 7, pp. 1697-1710, 2018.

[4] Gaud, Neha and Rathore, Maya and Suman and Ugrasen, "Human Gait Analysis and Activity Recognition: A Review," *2023 IEEE Guwahati Subsection Conference (GCON),* pp. 1-6, 2023.

[5] Yamamoto, Masataka and Shimatani, Koji and Ishige, uto and Takemura and Hiroshi, "Verification of gait analysis method fusing camera-based pose estimation and an IMU sensor in various gait conditions," *Scientific Reports,* vol. 12, 10 2022.

[6] Muro, Alvaro and Zapirain and Begoña and Mendez-Zorri, "ait Analysis Methods: An Overview of Wearable and Non-Wearable Systems, Highlighting Clinical Applications," *Sensors (Basel, Switzerland),* vol. 14, pp. 3362-94, 02 2014.

[7] Avellar, Letícia and Leal Junior and Arnaldo and Diaz, "POF Smart Carpet: A Multiplexed Polymer Optical Fiber-Embedded Smart Carpet for Gait Analysis," *Sensors,* p. 3356, 07 2019.

[8] Chambers, Henry and Sutherland and David, "A Practical Guide to Gait Analysis," *The Journal of the American Academy of Orthopaedic Surgeons,* vol. 10, pp. 222-31, 05 2002.

[9] Pirker, Walter and Katzenschlager and Regina, "Gait disorders in adults and the elderly: A clinical guide," *Wiener klinische Wochenschrift,* vol. 129, 10 2016.

[10] Rueterbories, Jan and Spaich, Erika G. and Larsen, Birgit and Andersen and Ole, "Methods for gait detection and analysis in ambulatory systems," *Medical engineering & physics,* vol. 32, pp. 545-52, 04 2010.

[11] U. Keisuke , A. Penny R. , N. M. Fiorentino and . A. Andrew E, "Hip rotation during standing and dynamic activities and the compensatory effect of femoral anteversion: An in-vivo analysis of

asymptomatic young adults using three-dimensional computed tomography models and dual fluoroscopy," *Gait & Posture,* vol. 61, pp. 276-281, 2018.

[12] Warmerdam, Elke and Romijnders, Robbin and Welzel, Julius and Hansen, Clint and Schmidt, Gerhard and Maetzler and Walter, "uantification of Arm Swing during Walking in Healthy Adults and Parkinson's Disease Patients: Wearable Sensor-Based Algorithm Development and Validation," *Sensors,* p. 105963, 2020.

[13] M. Pieter, S. M. Bruijn and Jacques, "The how and why of arm swing during human walking," *Gait & Posture,* vol. 38, no. 4, pp. 555-562, 2013.

[14] Sant'Anna, Anita and Wickström and Nicholas, "Symbolic Approach to Motion Analysis: Framework and Gait Analysis Case Studies," pp. 557-602, 01 2013.

[15] R. Aravinda, R. Marko , L. Yuguang , H. Songbo, F. Yihai , K. Kourosh , P. Marimuthu and N. Tuan , "Real-time monitoring of construction sites: Sensors, methods, and applications," *Automation in Construction,* vol. 136, p. 104099, 2022.

[16] "Accelerometer Sensor," Arduino, [Online]. Available: https://sensorkit.arduino.cc/sensorkit/module/lessons/lesson/09-the-accelerometer-sensor. [Accessed 17 09 2024].

[17] R. Lei , . J. Richard K. and H. David , "Whole body inverse dynamics over a complete gait cycle based only on measured kinematics," *Journal of Biomechanics,* vol. 41, no. 12, pp. 2750-2759, 2008.

[18] Çelik, Yunus and Stuart, Samuel and Woo, Wai Lok and Godfrey and Alan, "Wearable Inertial Gait Algorithms: Impact of Wear Location and Environment in Healthy and Parkinson's Populations," *Sensors,* 09 2021.

[19] Ekdahl, Mitchell and Loewen, Alex and Erdman, Ashley and Sahin, Sarp and Ulman and Sophia, "Inertial MeasIurement Unit Sensor-to-Segment Calibration Comparison for Sport-Specific Motion Analysis," *Sensors,* vol. 23, p. 7987, 09 2023.

[20] Z. Tobias , T. Bertram and B. Gabriele , "IMU-to-Segment Assignment and Orientation Alignment for the Lower Body Using Deep Learning," *Sensors (Basel, Switzerland),* vol. 18, 2018.

[21] Azdy, Rezania and Darnis and Febriyanti, "Use of Haversine Formula in Finding Distance Between Temporary Shelter and Waste End Processing Sites," *Journal of Physics: Conference Series,* vol. 1500, p. 012104, 04 2020.

[22] Chin, Robin and Hsiao-Wecksler, Elizabeth and Loth, Eric and Kogler, Geza and Manwaring, Scott and Tyson, Serena and Shorter, Kenneth and Gilmer and Joel, "A pneumatic power harvesting ankle-foot orthosis to prevent foot-drop," *Journal of neuroengineering and rehabilitation,* p. 19, 07 2009.

[23] W. Xingchen , K. Maria , R. Danijela , Durrant, S. Matthias and Axel, "Monitoring of gait performance using dynamic time warping on IMU-sensor data," *2016 IEEE International Symposium on Medical Measurements and Applications (MeMeA),* pp. 1-6, 2016.

[24] Zhu, Jia-Xin and Wang, Weifeng and Huang, Shiping and Ding and Wei, "An Improved Calibration Technique for MEMS Accelerometer-Based Inclinometers," *Sensors,* vol. 20, p. 452, 01 2020.

[25] Galor, Noam , Zeilig, Gabriel and Plotnik and Meir, "A New Measure for Quantifying Four-Limb Coordination of Human Gait Based on Mobility Sensors," *Sensors,* 09 2024.

[26] O. Theresa, "Kinematics and kinetics of gait," MEDICOL, 2020.

[27] Chan, Carl W, Rubins and Andrew, "Foot Biomechanics During Walking and Running," vol. 69, no. 0025-6196, pp. 448-461, 0501 1994.

[28] R. Andersson, B.-G. Javier, A. Rafael, C. Mikael and C. José, "Smartphone IMU Sensors for Human Identification through Hip Joint Angle Analysis," *Sensors (Basel, Switzerland),* vol. 24, no. 15, p. 4769, 2024.
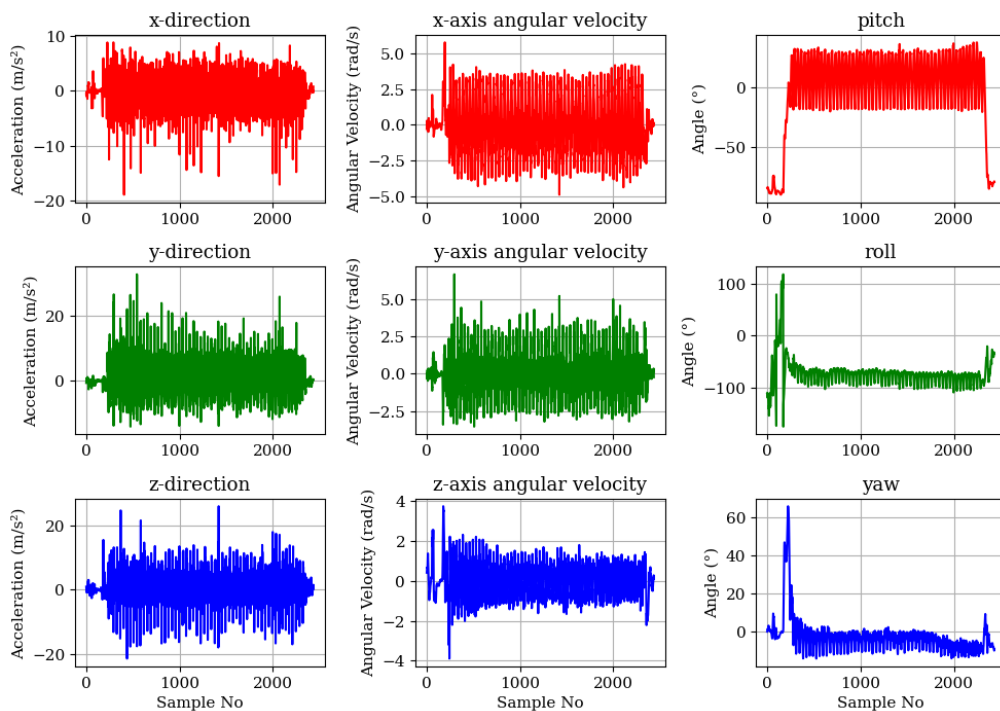
APPENDICE

Appendices A1: Kotlin Code

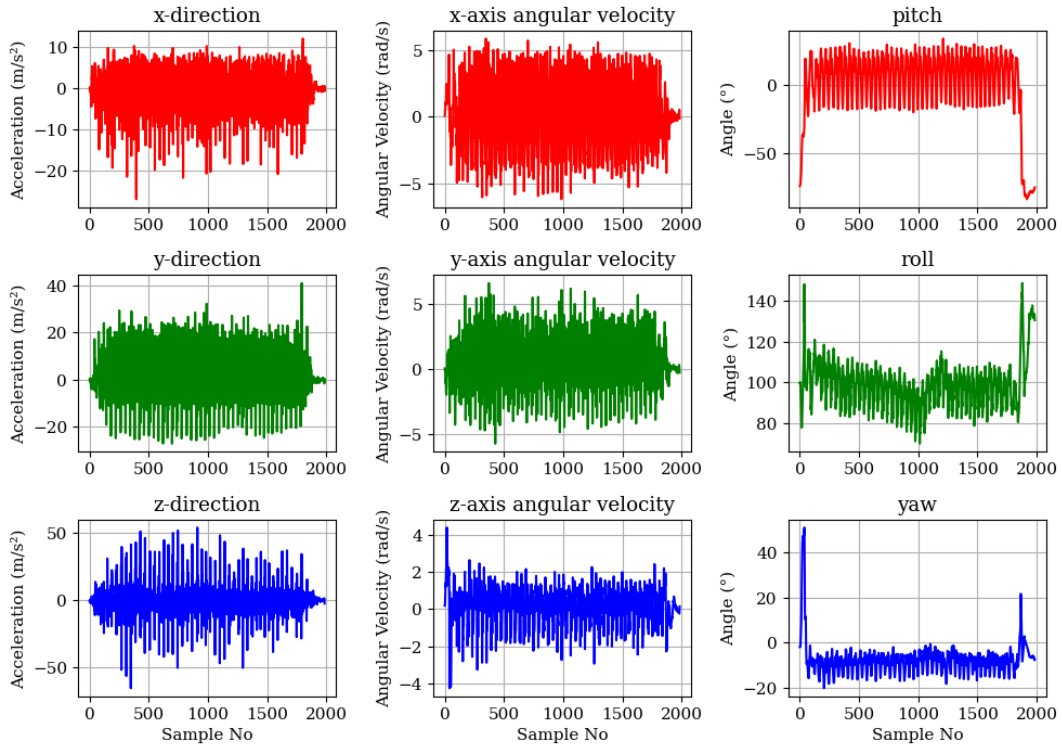| Mobile Application Data Retrieving Model |
|---|
| https://github.com/Osca-K/Person-Motion-Measurement-App |

Appendices B1: Raw Data
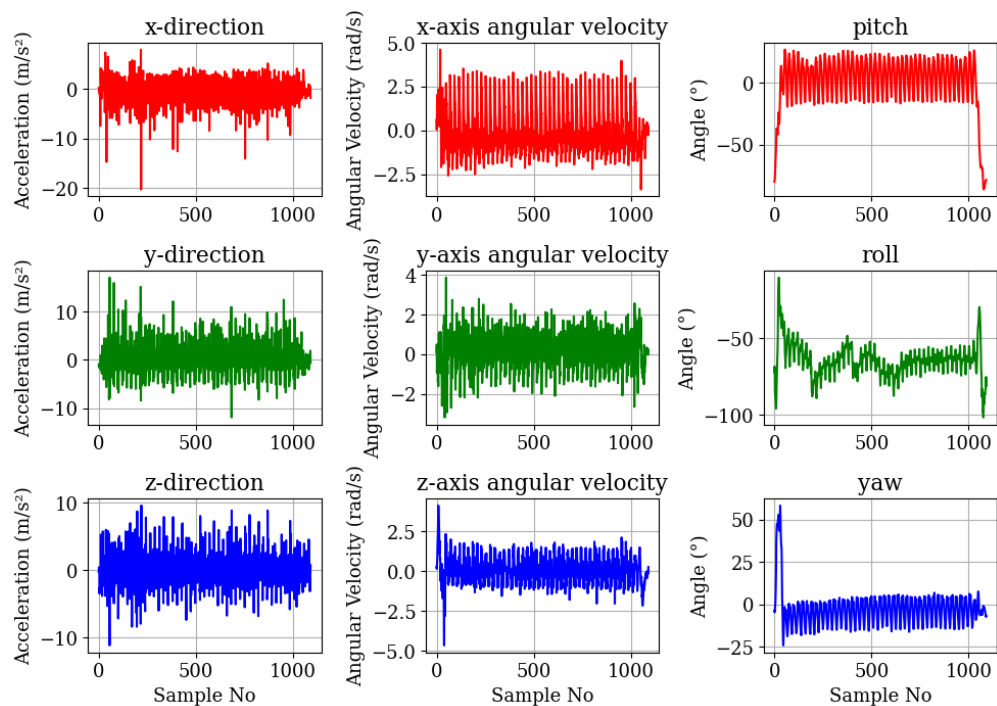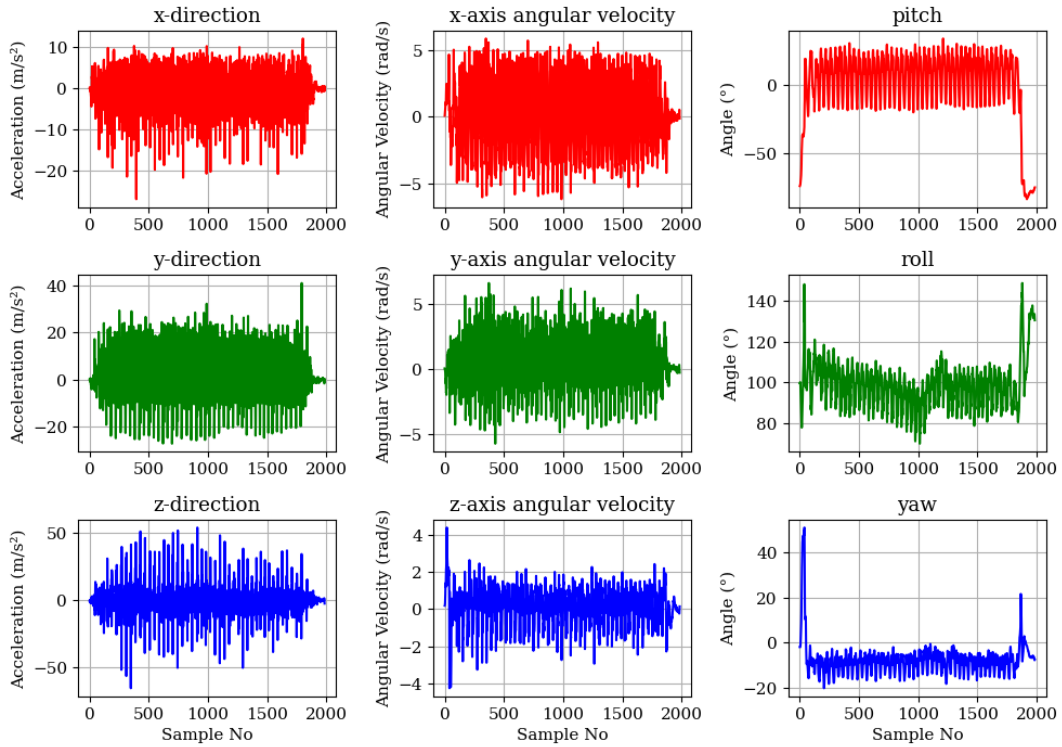

Relaxed walking with mobile in pocket
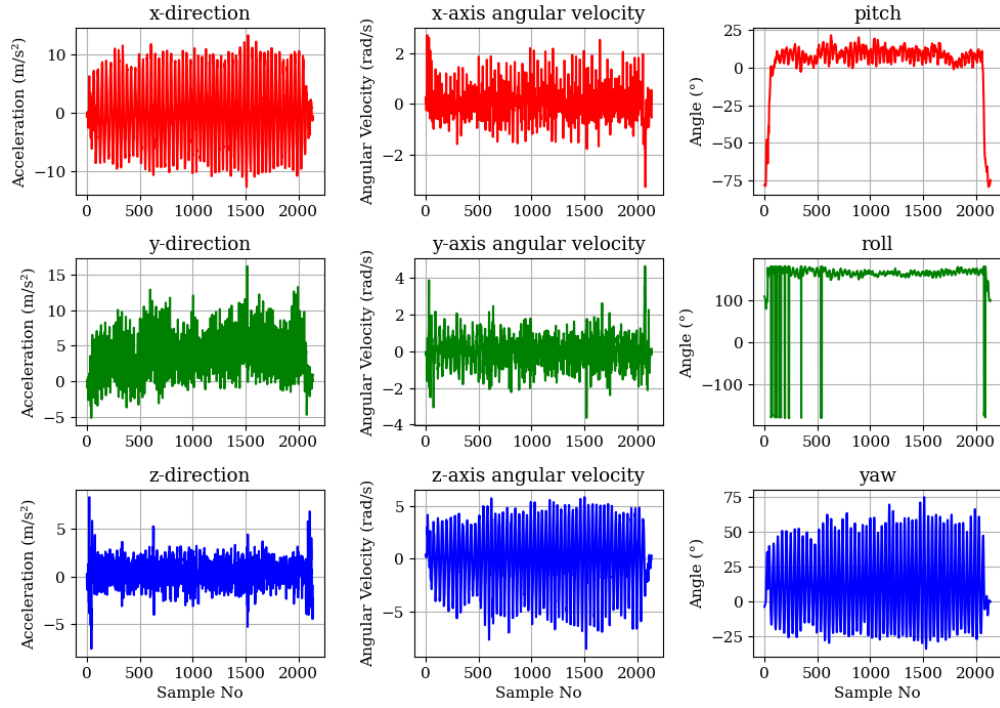

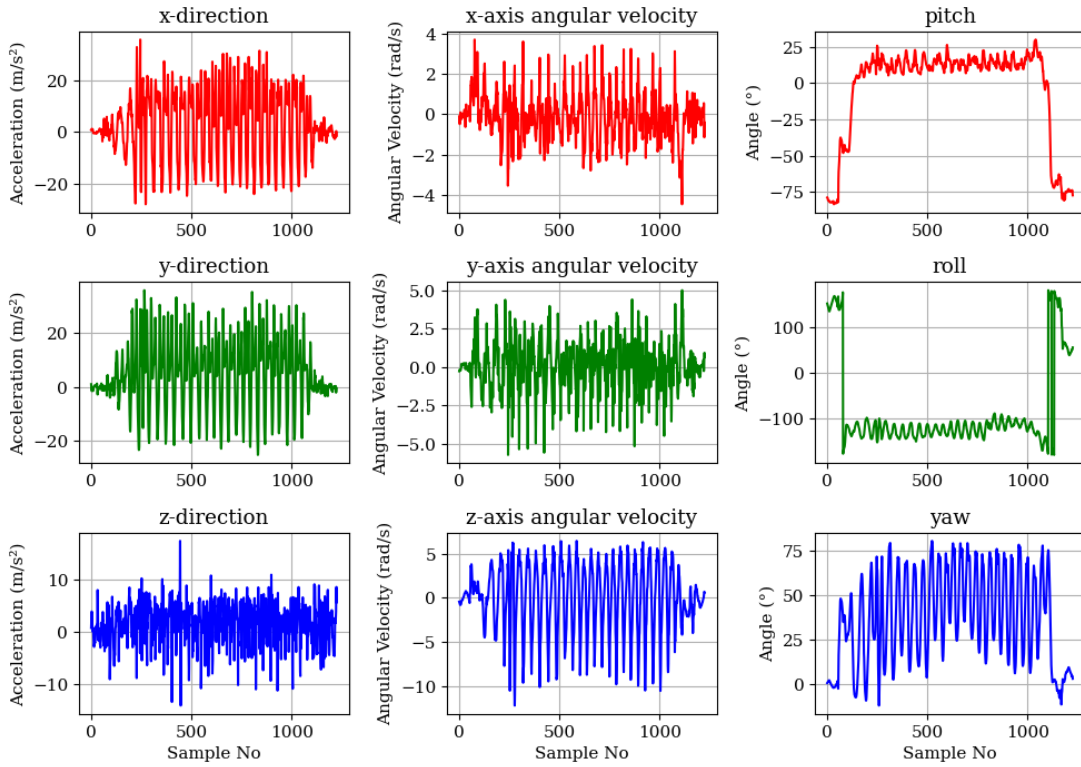Fast walking with mobile in pocket

Jogging walking with mobile in pocket

Relaxed walking with mobile in hand

Jogging walking with mobile in pocket

Relaxed walking with mobile in hand